From DEPARTMENT OF CLINICAL NEUROSCIENCE
Karolinska Institutet, Stockholm, Sweden

IN VIVO IMAGING MARKERS FOR THE CHARACTERIZATION OF MOLECULAR CHANGES IN PARKINSON AND HUNTINGTON´S DISEASE

Patrik Fazio

Stockholm 2017

Cover Illustration:

The image composition presented in the cover page is a top view of a 3D **brain** associated with an **Ensō** that symbolizes creativity but also the imperfection.
3D image generated by Ilias Bergström.

Published by Karolinska Institutet.
Printed by E-Print AB 2017

ISBN 978-91-7676-680-4

This thesis is dedicated to patients who suffer, for those will suffer from Parkinson and Huntington’s Disease and for the sake of knowledge.

When the mind is at Peace

When the mind is at peace,

the world too is at peace.

Nothing real, nothing absent.

Not holding on to reality,

not getting stuck in the void,

you are neither holy nor wise, just

an ordinary fellow who has completed his work.

P'ang Yun (Layman P’ang)

English version by Stephen Mitchell

IN VIVO IMAGING MARKERS FOR THE CHARACTERIZATION OF MOLECULAR CHANGES IN PARKINSON AND HUNTINGTON´S DISEASE

THESIS FOR DOCTORAL DEGREE (Ph.D.)

By

Patrik Fazio

Principal Supervisor:
Associate Professor Andrea Varrone
Karolinska Institutet
Department of Clinical Neuroscience

Co-supervisor(s):
Professor Lars Farde
Karolinska Institutet
Department of Clinical Neuroscience

Professor Christer Halldin
Karolinska Institutet
Department of Clinical Neuroscience

Professor Per Svenningsson
Karolinska Institutet
Department of Clinical Neuroscience

Opponent:
Professor Vesna Sossi
University of British Columbia, Vancouver
Physics Department

Examination Board:
Associate Professor Joakim Bergström
University of Uppsala
Department of Public Health and Caring Sciences

Associate Professor Oskar Hansson
Lund University
Department of Clinical science

Associate Professor Mark Lubberink
University of Uppsala
Department of Surgical Sciences, Radiology

ABSTRACT

Parkinson's disease (PD) and Huntington's disease (HD) are neurodegenerative disorders characterized by a progressive multi-systemic accumulation of misfolded proteins associated with neuronal dysfunction and neuronal loss. The rationale of this thesis is to examine, by means of the state of the art Positron emission tomography (PET) methodology combined with the use of high resolution MRI image molecular changes associated to the early stages of PD and HD. PET is a molecular imaging technique that, due to recent advancements in terms of radioligand development and PET instrumentation, such as the high-resolution research tomograph (HRRT) and PET quantification, may contribute to examine *in vivo* the distribution and availability of different biochemical targets. The work included in the thesis can be subdivided into two projects.

The first project is dedicated to PD and to the study of two relevant molecular targets (dopamine and serotonin transporters), examined respectively with the radioligands [^{18}F]FE-PE2I and [^{11}C]MADAM. In paper **I**, it is shown that [^{18}F]FE-PE2I represents a reliable imaging biomarker to study the dopamine transporter (DAT) in the striatum and in the substantia nigra in PD. In paper **II**, a validation of a new approach to examine the serotonin transporter protein in small brainstem structures is presented. In paper **III**, [^{18}F]FE-PE2I was used to study the entire nigro-striatal dopaminergic system, including dopamine projections, in a larger group of PD patients. The study was able to show a prominent involvement of the dopamine transporter in the striatum, a relatively milder reduction of DAT in the substantia nigra and a relative preservation of the protein along the nigro-striatal projections.

The second project is dedicated to the evaluation of Phosphodiesterase 10A as new molecular target for HD. This project includes two studies in which the radioligand [^{18}F]MNI-659 has been used as radioligand for PDE10A and the $D_{2/3}$ receptors radioligand [^{11}C]raclopride that has been used as internal reference. In paper **IV**, it is shown that aging is associated with a considerable reduction of PDE10A. In Paper **V**, the same targets are examined in selected cohorts of HD subjects in pre-manifest and manifest stages. The study shows that PDE10A was preserved in early pre-manifest HD subjects and progressively decreased in late pre-manifest and manifest HD stages.

In conclusion the presented applications of new PET molecular imaging probes provided relevant information that contributes to measure early changes of molecular targets associated with the onset and progression of neuronal loss occurring in PD and HD.

LIST OF SCIENTIFIC PAPERS

I. **Fazio P**, Svenningsson P, Forsberg A, Jönsson EG, Amini N, Nakao R, Nag S, Halldin C, Farde L, Varrone A. Quantitative analysis of [^{18}F](E)-N-(3-Iodoprop-2-Enyl)-2β-Carbofluoroethoxy-3β-(4'-Methyl-Phenyl) Nortropane binding to the dopamine transporter in Parkinson's disease. J Nucl Med. 2015 Mar 19.

II. **Fazio P**, Schain M, Varnäs K, Halldin C, Farde L, Varrone A. Mapping the distribution of serotonin transporter in the human brainstem with high-resolution PET: Validation using postmortem autoradiography data. Neuroimage. 2016 Jun; 133:313-20.

III. **Fazio P**, Svenningsson P, Cselenyi Z , Halldin C, Farde L, Varrone A. In vivo mapping of nigro-striatal dopamine transporter availability in early Parkinson´s disease patients using [^{18}F]FE-PE2I and high-resolution positron emission tomography. Manuscript.

IV. **Fazio P**, Schain M, Mrzljak L, Amini N, Nag S, Al-Tawil N, Fitzer-Attas CJ, Bronzova J, Landwehrmeyer B, Sampaio C, Halldin C, Varrone A. Patterns of age related changes for phosphodiesterase type-10A in comparison withdopamine $D_{2/3}$ receptors and sub-cortical volumes in the human basal ganglia: a PET study with [^{18}F]MNI-659 and [^{11}C]raclopride with correction for partial volume effect. Neuroimage. 2017

V. **Fazio P**, Fitzer-Attas CJ, Bronzova J, Nag S, Warner JH, Landwehrmeyer B, Al-Tawil N, Halldin C, Mrzljak L, the PEARL study collaborators, Sampaio C and Varrone A. Imaging of phosphodiesterase 10 A (PDE10A) enzyme levels in the living human brain of Huntington’s disease gene expansion carriers and healthy controls with positron emission tomography. Manuscript.

LIST OF NON THESIS PUBLICATIONS

I. Nag S, **Fazio P**, Lehmann L, Kettschau G, Heinrich T, Thiele A, Svedberg M, Amini N, Leesch S, Catafau AM, Hannestad J, Varrone A, Halldin C. In Vivo and In Vitro Characterization of a Novel MAO-B Inhibitor Radioligand, [^{18}F]Labeled Deuterated Fluorodeprenyl. *J Nucl Med.* 2016 Feb; 57(2):315-20.

II. Sonni I, **Fazio P**, Schain M, Halldin C, Svenningsson P, Farde L,Varrone A. Optimal Acquisition Time Window and Simplified Quantification of Dopamine Transporter Availability Using [^{18}F]FE-PE2I in Healthy Controls and Parkinson Disease Patients. *J Nucl Med*. 2016 Oct;57(10):1529-1534.

III. Sturm S, Forsberg A, Nave S, Stenkrona P, Seneca N, Varrone A, Comley RA, **Fazio P**, Jamois C, Nakao R, Ejduk Z, Al-Tawil N, Akenine U, Halldin C, Andreasen N, Ricci B. Positron emission tomography measurement of brain MAO-B inhibition in patients with Alzheimer's disease and elderly controls after oral administration of sembragiline. *Eur J Nucl Med Mol Imaging*. 2017 Mar;44(3):382-391.

IV. Delnomdedieu M, Forsberg A, Ogden A, **Fazio P**, Yu CR, StenkronaP, Duvvuri S, David W, Al-Tawil N, Vitolo OV, Amini N, Nag S, Halldin C, Varrone A. In vivo measurement of PDE10A enzyme occupancy by positron emission tomography (PET) following single oral dose administration of PF-02545920 in healthy male subjects. *Neuropharmacology*. 2017 Jan 22.

V. Schain M, Cselenyi Z, **Fazio P**, Arakawa R, Rosenqvist G, Halldin C, Farde L,Varrone A.Validation of a Partial Volume Effect Correction of brain PET Data Based on FreeSurfer and AAL Segmentation. Submitted.

VI. Schain M, **Fazio P**, Mrzljak L, Amini N, Al-Tawil N, Fitzer-Attas C, Bronzova J, Landwehrmeyer B, Sampaio C, Halldin C, Varrone A. Revisiting the Logan Plot to account for non-negligible blood volume in brain tissue. Manuscript.

VII. Paucar M,Engvall M, Söderhäll C, Skorpil, **Fazio P**, Lagerstedt-Robinson K, Solders G, Skoog T, Zhang X, Freyer C, Wredenberg A, Angeria M, Varrone A, Nennesmo I, Risling M, Jaio H, Wedell and Svenningsson P. Broad spectrum and widespread neurodegeneration associated with spino cerebellar ataxia type 4. Manuscript.

TABLE OF CONTENTS

1 INTRODUCTION....1
1.1 Movement disorders and basal ganglia....1
1.2 Positron emission tomography....4
1.2.1 Image and data acquisition....4
1.2.2 Regional, template or voxel based analysis of PET Data....6
1.2.3 Principles of quantification of radioligand binding....7
1.2.4 Parametric images....9
1.3 Molecular neuroimaging in movement dIsorders....10
1.3.1 Parkinson's Disease....11
1.3.2 Huntington's disease....16
2 AIMS....21
3 Methodological consideration....22
3.1 Positron emission tomography....22
3.2 Magnetic resonance imaging....22
3.3 In vitro autoradiography studies....23
3.4 Kinetic modeling and outcome measures....23
3.5 Partial Volume effect and correction....24
3.6 Tailored template-based analysis using parametric images....25
3.7 Recruitment and characteristics of Parkinson and Huntington's disease patients....27
4 Results and Reflections....29
4.1 Paper I....29
4.1.1 Evaluation of [^{18}F]FE-PE2I as radioligand for DAT imaging *in vivo* in PD patients and in healthy controls.....29
4.2 Paper II....31
4.2.1 Quantification of 5-HTT binding in small nuclei of the brainstem: a validation of a template based approach.....31
4.3 Paper III....33
4.3.1 DAT availability in the substantia nigra, axons and striatal terminals in early PD patients....33
4.4 Paper IV....35
4.4.1 Age related reduction of PDE10A availability in the basal ganglia....35
4.5 Paper V....37
4.5.1 Examination of PDE10A availability across a broad spectrum of HD stages....37
5 Future perspectives....39
6 Acknowledgments....41
7 References....43

LIST OF ABBREVIATIONS

AADC	Aromatic aminoacid decarboxylase
AD	Alzheimer´s disease
ARG	Autoradiography
BP_{ND}	Non displaceable Binding Potential
CAG	Cytosine-adenine-guanine
cAMP	cyclic adenosine monophosphate
cGMP	cyclic guanosine monophosphate
CSF	Cerebrospinal fluid
3D	Three dimensional
4D	Four dimensional
DAT	Dopamine transporter protein
$D_{2/3}$	Dopamine 2 and 3 receptors
DBS	Disease Burden score
DLB	Dementia with Lewy bodies
DOPA	Dihydroxyphenylalanine
FWHM	Full-width half-maximum
GABA	Gamma-amino butyrric acid
GM	Grey matter
GPe	External segment of the globus pallidus
GPi	Internal segment of the globus pallidus
HD	Huntington’s Disease
HDGEC	Huntington’s Disease gene expansion carrier
HRRT	High Resolution Research Tomograph
5-HTT	5-hydroxytriptamine transporter, serotonin transporter
LB	Lewy bodies
LSO	Lutetium Oxyorthosilicate
MNI	Montreal Neurological Institute
MSNs	Medium-sized spiny neurones

MRI	Magnetic Resonance imaging
mHTT	Mutant huntingtin
MSA	Multiple system atrophy
OSEM	Ordered-subset expectation maximization
PD	Parkinson’s Disease
PDE10A	Phosphodiesterase 10 A
PET	Positron Emission Tomography
PSP	Progressive supranuclear palsy
PVE	Partial Volume effect
PVEc	Partial Volume effect correction
ROI	Region of interest
SRTM	Simplified reference tissue model
SWEDD	Scan without evidence of dopaminergic deficit
TAC	Time-activity curve
1-TCM	One-tissue compartment model
2-TCM	Two-tissue compartment model
UPDRS	Unified Parkinson’s disease rating scale
UHDRS	Unified Huntington’s disease rating scale
VMAT2	Vesicular monoamine transporter type 2
V_{ND}	Non-displaceable distribution volume
VOI	Volume of interest
V_T	Total distribution volume
WAPI	Wavelet-aided parametric imaging
WM	White matter

1 INTRODUCTION

1.1 MOVEMENT DISORDERS AND BASAL GANGLIA

Movement disorders are a group of central nervous system's syndromes characterized by an impairment of voluntary movements, abnormal muscle tone, involuntary movements and abnormal postures and postural reflexes. There are two main categories: hyperkinetic movement disorders characterized by an excess of involuntary movements and hypokinetic movement disorders in which a global reduction of movement is present.

Movement disorders were traditionally related to dysfunction of the extra-pyramidal system which is composed by different central nervous system structures (basal ganglia, cerebellum, and different thalamic nuclei) and pathways (nigrostriatal, striato cortical) involved in the modulation and regulation of movement.

Basal ganglia are the anatomical structures mostly involved in movement disorders. They are grey matter structures located medially and deeply in the encephalon, characterized by dense internuclear projections. Basal ganglia receive inputs from all cortical areas (sensory, motor, and associative) and produce a much lower number of outputs mainly back to the cortex and in minor extent to the brainstem and cerebellum (1,2). Five parallel and closed circuits have been proposed (motor, oculolomotor, dorsolateral prefrontal, lateral orbitofrontal and limbic). It is now generally agreed that these loops follow a functional and structural organization with subdivisions into sensorimotor, associative, and emotional functions (3). In this functional organization one of the major roles of basal ganglia appears to be in mediating automatic activities.

Different brain structures compose the basal ganglia:

a) The **striatum** that is composed by the caudate nucleus, the putamen and by the nucleus accumbens. The striatum represents the main input structure of the basal ganglia circuit.
b) **Globus pallidus pars interna (GPi**) **and externa (GPe**). The pars interna is the main output structure of the basal ganglia circuit.
c) The **substantia nigra** pars compacta (cell dense pigmented regions) and the pars reticulata (unpigmented). The main source of dopamine innervations is found in the substantia grigia pars compacta.

Connected to this functional core there are other associated nuclei

d) Ventro-lateral nuclei of the thalamus.
e) Subthalamic nuclei of Luys.

Striatal GABAergic medium spiny neurons (MSNs) densely receive dopaminergic input from the substantia nigra and other input from cortical and thalamic projections. Those neurons integrates information from the substantia nigra and project to other connected interface nuclei and to the rest of the brain (2). GPi is the most important basal ganglia interface structure. It facilitates thalamic inhibition and consequently modulates the cortex using excitatory (glutamatergic) synaptic connections.

Two major pathways are traditionally described between the striatum and the GPi and are part of the 3 functional systems described above (sensorimotor, associative and emotional)

1. A **direct pathway** which is inhibitory and modulates directly the substantia nigra pars reticulata and the subthalamic nucleus.
2. An **indirect pathway** which is excitatory and modulates the GPi with a multisynaptic circuit that reaches the interface (GPi) through an intermediate connection with the GPe.

The direct pathway provides a direct inhibition whereas the indirect pathway provides a thalamic excitation through disinhibition. Traditionally the direct pathway should promote the movement whilst the indirect pathway should reduce it (4). A molecular distinguishing feature of the two pathways is the differential expression of dopamine receptors. D_1 dopamine receptors are selectively expressed in the direct pathway, whereas in the indirect pathway mostly D_2 receptors are expressed. Despite the mentioned molecular and functional differentiation some preclinical data recently supported the idea that both intrastriatal connections (direct and indirect) work dynamically in concert depending on the form of the synaptic plasticity expressed with a given motor action (5). The classic schematic description of basal ganglia circuitries has contributed to characterize the role of dopamine in the modulation of different basal ganglia structures but it represents an oversimplification of the basal ganglia complexity (6).

Nowadays, the close link between basal ganglia function and the control and modulation of motor functions have expanded to account a broad sets of non motor functions in which the basal ganglia are involved such as cognition, learning and behavior (7-9).

The traditional description does not take into account the complexity that might be added if the contribution of other players is considered. For instance, other neurotransmitter systems are also involved in the regulation of the basal ganglia circuits (10-12). The striatum appears to be

functionally sub-compartmentalized in striosome and matrix with distinct neurochemical organization that have an impact on dopamine dynamics and striatal synaptic functions (13).The subthalamic nucleus is also an important supplementary input structure (cortico-subthalamic-pallidal hyper-direct pathway) (14).

The mentioned complexity is furthermore sustained by different patterns of electrophysiological activities in the different striatal nuclei (15). In particular synchronized neural oscillations in the beta and gamma frequency may contribute to regulate and optimize network functionalities and dopamine release. In PD for example, an excess of synchronization has been recently described (16).

The traditional models might also contribute to the understanding of some aspects of the motor symptoms that occur in movement disorders but it becomes less complete when other important features of movement disorders are considered. In fact, so far, movement disorders have been traditionally associated to the dysfunction of the motor circuit of the basal ganglia. Hypokinetic features of movement disorders (i.e. bradykinesia in parkinsonism) have been explained by the progressively reduced dopamine stimulation. The decrease in dopaminergic input would generate a reduced inhibition of the indirect pathway and a decreased excitation of the direct pathway, resulting in a final increase of the thalamic inhibitory activity to the premotor and motor cortical areas. On the other hand, the predominant reduction of signaling in the indirect pathway has been linked to the reduced suppression of involuntary movements (chorea) that occurs in Huntington's disease (4).

The ground for the co-existence of hyperkinetic and hypokinetic features is still under investigation in some disorders such as in HD and advanced PD. Moreover, it has been considered "a paradox" the positive consequences that occurred after focal lesions in basal ganglia regions (i.e. thalamotomy, pallidotomy, subthalatomy) which have been performed with stereotaxic surgery (17,18). This might also be connected with the complexity, dynamic and integration of the signaling of basal ganglia with the rest of the brain.

Future investigations might shed some light on the mentioned limitation of those models and may contribute to explain the clinical variability of motor, behavioral and cognitive symptoms observed in patients with movement disorders.

PET molecular imaging represents a useful tool to evaluate and characterize the role of different molecular targets involved in the modulation of basal ganglia circuits.

1.2 POSITRON EMISSION TOMOGRAPHY

Positron Emission tomography (PET) is an *in vivo* molecular imaging technique able to examine the distribution and concentrations of radiolabeled compounds binding to different molecular targets. Radiolabeled compounds are referred to as radioligands. In recent years ~ 400 targets have been evaluated and ~ 40 radioligands were developed and applied *in vivo* for PET studies of the human brain. For research or clinical purposes PET has been used to measure the blood flow, glucose metabolism, receptor density and enzyme activities. The basic principle of PET stands on the measurement of emitting annihilation photons that are generated from the decay of positron-emitting or isotopes (^{18}F,^{11}C,^{13}N,^{15}O). Positrons emitted in matter lose most of their kinetic energy until an interaction by annihilation with an electron of the surrounding matter (i.e. brain parenchyma) occurs. The annihilation produces a pair of photons (gamma rays) with a known energy (~ 511 KeV) and direction (180 º) that are detected and recorded simultaneously by scintillation crystals (the basic detector hardware of a PET system) for the entire duration of the PET acquisition (Figure 1).

1.2.1 Image and data acquisition

A dynamic PET study consists in a continuous measurement of the emitted radioactivity (coincidences) in a period of time that varies among different radioligands (commonly 60-90 minutes). A PET radioligand is administered intravenously to the subjects and in this way enters into the circulation. From the venous blood stream the radioligand arrives to the heart chambers and then is distributed into the arterial circulation (Figure 1). After 10-15 seconds the radioligand arrives at the capillary bed where exchanges with the tissue begin to take place. A fraction of the radioligand is extracted from blood to the tissue and a fraction (depending of its reversible or irreversible behavior) leaves the tissue and returns into the main circulation. In the target tissue such as the brain, in this manner, the concentration of radioligand changes over time and the radioactivity is detected by measuring the number of events generated by the annihilation of positrons with electrons (Figure 1).

The collected data are subdivided into frames of different durations that are physiologically coherent with the fate of the radioactivity in the specific target. At the end of the acquisition the detected information (the projections of the pair of photons) is reconstructed by dedicated algorithms in order to create 3D images for each time frame.

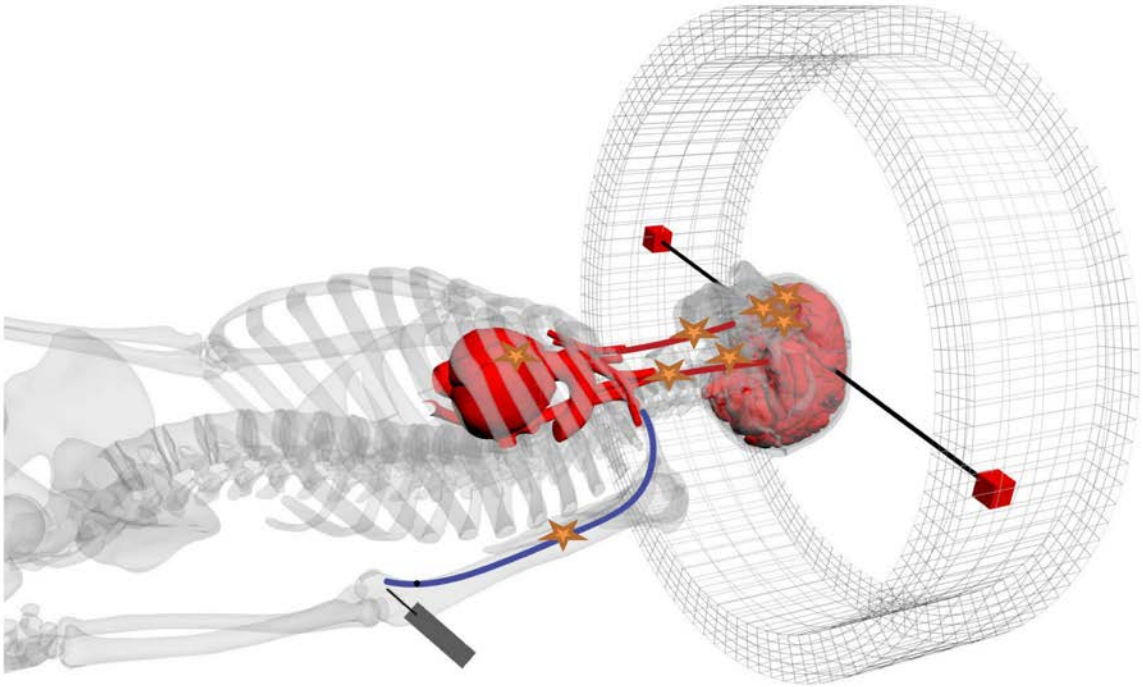

Figure 1. Image depicting the fate of a given radioligand after an intravenous injection. When the molecular target is reached the annihilation phenomena occurs and the pairs of photons are detected by the PET system.

From the reconstructed dynamic sequence of images it is possible to derive time activity curves (TACs) that are usually extracted from a volume of interest (VOI) in the brain and by measuring the average volumetric concentration of radioactivity at each time frame (Figure 2).
Another important requirement for a proper quantification of a radioligand is the measurement of radioactivity in the circulating blood (plasma and whole blood) and the generation of the so called arterial input function, that is the plasma concentration of unchanged radioligand over time. The input function is obtained by multiple samples of the arterial blood after cannulation of the radial artery, followed by separation of plasma from blood cells and measurement of the fraction of unchanged parent and metabolites with high-performance liquid chromatography.

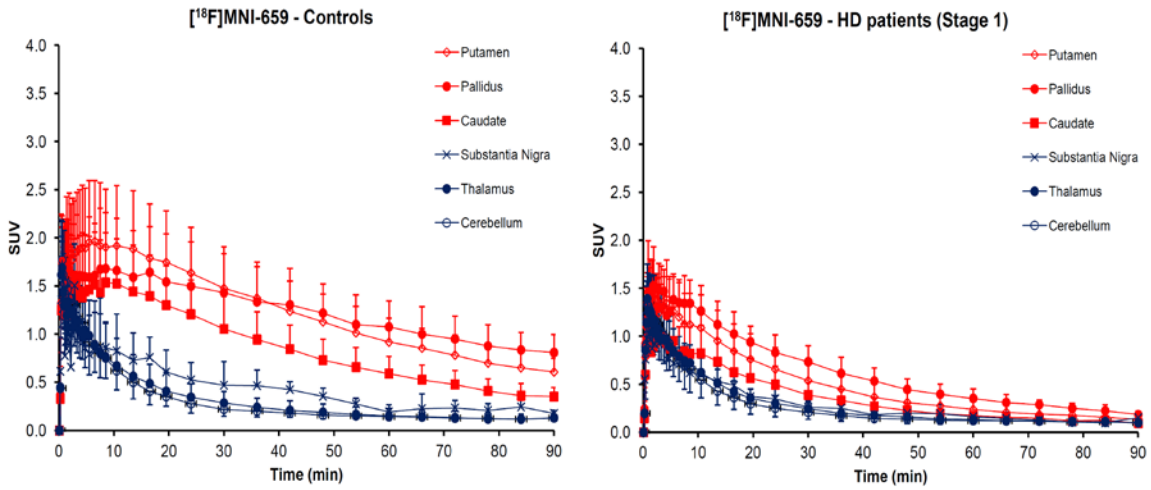

Figure 2. Average standardized uptake value (SUV) time activity curves of a reversible radioligand ([^{18}F]MNI-659) in healthy controls subjects and in stage 1 HDGECs in a several regions of interest.

1.2.2 Regional, template or voxel based analysis of PET Data

When the 4D images are available, a set of VOIs are usually defined in order to extract the TACs that are used for the quantification of PET data. Different approaches are available for the definition of the VOIs and the choice is dependent on the specific study and on the target availability.

The most common approach is the manual delineation of anatomical regions of interest upon MRI images. A prerequisite to manually define regions of interest (ROIs) is that the region should be clearly identifiable in the MRI images based on the presence of known anatomical landmarks. Some of the requisites are based upon a clear regional delimitation, a homogenous tissue composition (image intensity), and spatially heterogeneous MRI imaging properties. This procedure is time consuming and generally sensitive to biases due to differences between users.

Another approach is to use automatic methods to define ROIs on MRI images. Different software packages for brain PET applications are now available and validated. These approaches utilize a priori anatomical information obtained from validated probabilistic brain atlases or anatomical parcellation strategies to assign anatomical labels to each MRI voxel. The set of preprocessing tools offered by the Freesurfer package (http://surfer.nmr.mgh.harvard.edu) represents a valid example of an automatic approach also used in two of the studies presented in this thesis (IV- IV). The technical details of pre-processing of MRI images are described in prior publications (19,20).

For the generation of subcortical ROIs a section (volume based stream) of the Freesurfer pipeline is dedicated to the volumetric segmentation of the brain and to the labeling of tissue classes. The algorithm is based upon the existence of an atlas containing probabilistic information on the location of structures and on the subject specific measured value (21). This atlas and the relative spatial coordinates were obtained with a manually labeled training set of high-resolution MR images of 39 subjects. The advantage of this implementation is that it relies on a registration procedure that takes in account the anatomical variability including possible consequences of degeneration processes such as atrophy.

1.2.3 Principles of quantification of radioligand binding

The objective of quantification of radioligand binding is to generate physiologically relevant parameters able to describe and quantify radioactivity measurements of biological targets in the brain (receptor concentration, transporter protein availability, enzyme levels or activity and metabolic parameters) obtained with PET measurements. The biochemical fate of a radioligand and the relative tissue radioactivity concentration data are influenced by several factors such as plasma protein binding, permeability of the blood brain barrier, tissue blood flow, rate of the extraction of the tracer from the capillary, binding association and dissociation rates, non specific tissue binding and by the eventual presence of radioligand metabolites. In the current practice, mathematical models are employed to describe the precise relationship between the *in vivo* radioligand behavior and a set of parameters of interest in brain target tissues (22).

In the studies presented in this thesis the kinetic of the radioligand is described by compartmental models that allow the estimation of exchange rates (rate constants) among tissue compartments (Figure 3). Those models assume that the injected radioligand will, at any given time, move and exist in one of the compartments, that each compartment is homogenous without concentration gradients and that the fractional rate of change of concentration in one compartment remains constant during the duration of the PET acquisition.

From the estimation of the rate constants between compartments and from the known input function other macroparameters of interest are calculated such as the total distribution volume (V_T) which is the ratio of the tissue concentration to the plasma concentration (input function) at equilibrium (22). Examples of compartmental models are presented in figure 3 below.

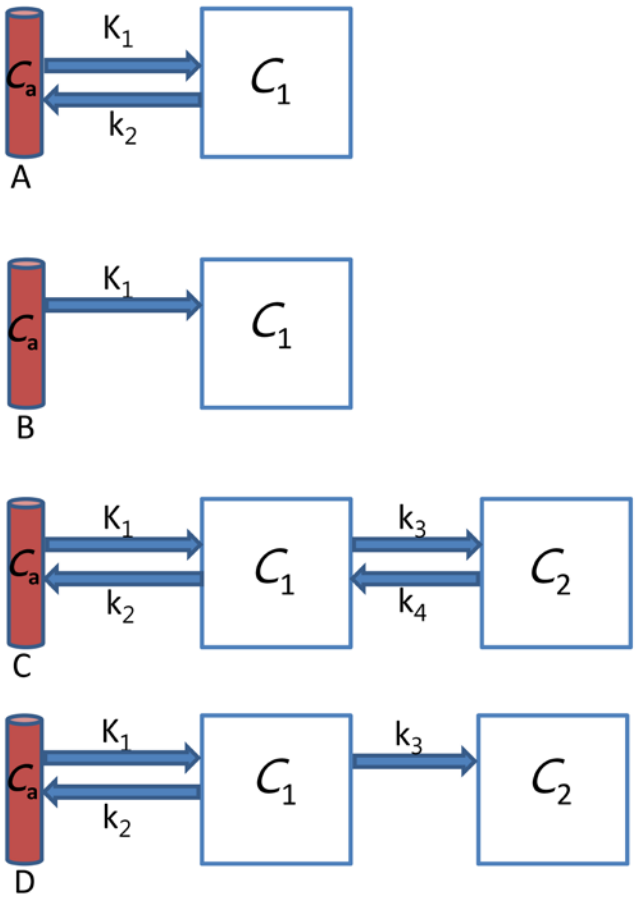

Figure 3. Compartmental models. ***C*a** is the concentration of tracer in arterial plasma, C_1, C_2 are the tracer concentrations in compartments 1 and 2. $\mathbf{K_1}$, $\mathbf{k_2}$, $\mathbf{k_3}$ and $\mathbf{k_4}$ are the rate constants that define the rate of tracer exchange between compartments. A. One tissue compartment with irreversible uptake B. one tissue compartment with reversible tissue uptake C. Two tissue compartments with reversible uptake D. Two tissue compartments with irreversible uptake.

Other approaches are also available if inside the brain parenchima there is a region (a reference region) with a negligible amount of specific binding. The general idea is that a regional TAC becomes the reference of the model in substitution of the arterial input function (23). When possible, this approach is preferable since there is no longer need of the arterial cannulation and this considerably reduces the subject's discomfort during the study. Moreover, graphical adaptations of reference tissue models are also available (i.e. non-invasive Logan graphical analysis) (24). Models based on linear graphical analysis are in some instances more efficient for some radioligands and also tend to reduce the computational requirement that becomes useful when the model is applied at voxel level (i.e. parametric images). Another advantage of this approach is that the derived parameter of interest is the non-displaceable binding potential (BP_{ND}) which is a more specific measure of target availability. BP_{ND} is defined as the ratio between the specifically bound radioligand to the non-displaceable binding at equilibrium.

1.2.4 Parametric images

Another attractive approach to perform analysis of PET data is to perform parametric mapping. Parametric mapping approaches were established in order to estimate outcome measures of interest in each voxel that composes a PET image. As a result, 3D images with spatial maps of binding pattern expressed as outcome measure are generated. Different denoising strategies have been implemented and several attempts have been made to reduce the computational cost of measuring PET outcome measures at voxel level.
An example of parametric images obtained in the Parkinson's study with [^{18}F]FE-PE2I is shown in figure 4.

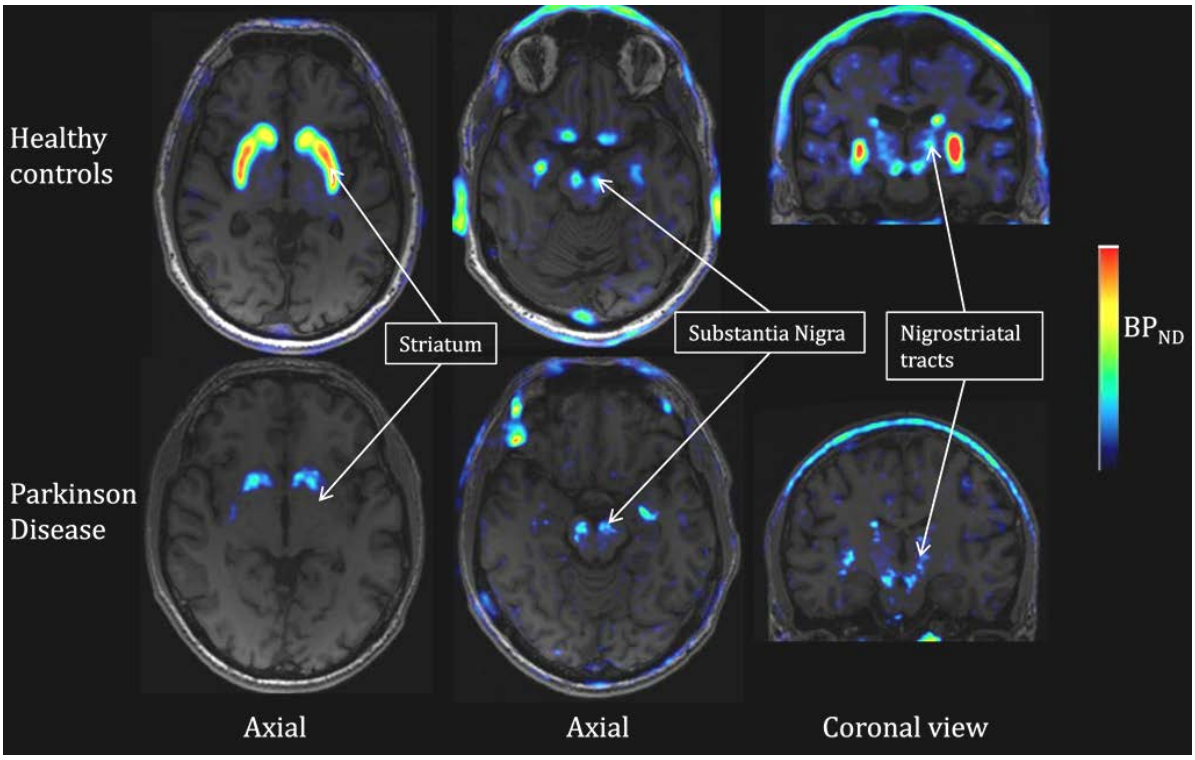

Figure 4. Representative DAT parametric images of [^{18}F]FE-PE2I in a control subject (upper panel) and in an early PD patient (stage 1.5 Hoehn & Yahr) (lower panel).

The method used at Karolinska Institutet PET Centre was developed in 2006 and it is based on a solution that uses a wavelet-based approach (25) The method also called wavelet-aided parametric imaging (WAPI) operates with the wavelet transformation to eliminate some known spatial frequencies (high frequencies) associated with the noise of a PET measurement. This approach have also been recently optimized to consider the PET system resolution and the reconstruction procedure (26).

1.3 MOLECULAR NEUROIMAGING IN MOVEMENT DISORDERS

Primary forms of movement disorders are caused by a neurodegenerative etiology. In the human brain the macroscopic consequence of a neurodegenerative process is characterized by accumulation of protein aggregates, neuronal loss (with or without atrophy) and gliosis. Pathological alterations can be examined in vivo by means of structural imaging or in vitro by post mortem histological studies. Post mortem studies were particularly successful to precisely describe common features of different neurodegenerative processes, such as protein misfolding aggregation and accumulation (27). Pathological filamentous protein aggregates were progressively characterized and became the postmortem diagnostic golden standard: β-amyloid characteristic in Alzheimer's disease (AD), hyperphosphorylated protein tau for Progressive Sopranuclear Palsy (PSP) and AD, α-synuclein for PD, Multiple System Atrophy (MSA) and dementia with Lewy bodies (DLB) and mutant huntingtin (mHTT) for Huntington's disease. Different disease phenotypes might be explained by the consequences of distinctive functions of native (non-misfolded) proteins, different patterns of accumulation (regional distribution in the brain) or subcellular localization (intracellular or extracellular) of misfolded protein aggregates and finally by particular vulnerabilities of a different specific neuronal systems.

The link between these pathological aggregates and neuronal apoptotic mechanisms has not been fully elucidated. Brain PET imaging represents a useful methodology to examine relevant *in vivo* characteristics, such as the distribution and availability of different biochemical targets in the diseased and healthy brain. In neurodegenerative disorders the general focus of PET imaging was traditionally focused on the study of dysfunctional molecular consequences related to different diseases. Several molecular targets have been explored with clinical PET studies such as different monoaminergic systems and relative receptors (dopamine, serotonin, cholinergic) and neurotransmitters (GABA, adenosine), regulatory intracellular enzymes (monoamine oxidase B, phosphodiesterase PDE4 and PDE10A), examination of cerebral blood flow and metabolism, neuroinflammation proteins (translocator protein) and last but not least in vivo protein accumulation patterns (beta-amyloid and tau). More recently, applications of molecular imaging techniques *in vivo* have focused on earlier phases of neurodegenerative processes which begin decades before a full phenotypic expression of the disease. Thus, dysfunctions of the molecular circuitries might be expected in preclinical and prodromal stages. With this perspective, one might also expect that the clinical and pharmacological management of patients affected by neurodegenerative disorders would benefit from the availability of reliable *in vivo* molecular biomarkers.

A possible application scenario could be that an imaging biomarker would be of great help to understand different clinical expressions or to support diagnostic workflows (i.e. differential diagnosis with atypical parkinsonisms, molecular stratification/enrichment of PD and HD individuals). Moreover, in an era in which the panel of disease-modifying therapies for neurodegenerative disorders is expanding (28-32) another potential application of early imaging biomarkers would be to monitor the disease progression and the efficacy of treatment when clinical outcomes may easily fail to produce relevant results (33,34).

1.3.1 Parkinson's Disease

Parkinson's disease (PD), at the time of the diagnosis, is clinically characterized by a progressive reduction of motor capacities with rigidity, hypokinesia, resting tremor, postural instability and an overall reduction of automatic movements. These typical motor signs are associated with a variegate set of non motor symptoms such as cognitive decline, autonomic dysfunctions, sleep related disorders and affective disorders. Non motor symptoms are becoming progressively more relevant for the medical and research communities because some of them initiate years before the clinical diagnosis (i.e. rapid eye movement [REM] sleep behavior disorders, constipation and olfactory dysfunctions) and may help to characterize a so called prodromal phase (35).

From a neurobiological perspective, PD is now seen more as a group of disorders with a characteristic dopamine deficit due to degeneration of the dopaminergic nigro-striatal system. PD is characterized by a multiform accumulation of alpha-synuclein rich aggregates, different genetic susceptibilities and various lifestyle risk factors (i.e. smoking, coffee, urate and the composition of gut microbiome) (36-39).

The genetic background of PD has recently been linked to mutations of different genes (i.e. alpha-synuclein, LRRK2, Parkin, PINK1, VPS35, DJ-1, ATP13A2, TMEM230) with autosomal dominant and recessive familial PD variants that account for 5-10% of cases (40). Moreover, in the majority of sporadic PD cases the disease may develop as a consequence of genetic susceptibility factors (polymorphisms in SNCA, LRRK2 and for heterozygous mutation in the GBA) (41,42). In some cases clinical correlations with Lewy pathology patterns have already been recognized (43) suggesting that the clinical heterogeneity might be sustained by a genetic substrate. The disease has a progressive course and patients usually experience a progressive decline of independence and a significant reduction of quality of life. The management of the disease is often challenging and becomes difficult in the advanced

stages of the disease. PD is the second most common neurodegenerative disorders with prevalence estimates that ranges between 100-300 per 100.000 (44-46). The burden for the society in term of care giving and finances is relevant if one considers that in Sweden there are approximately 20.000 people suffering from PD (47) and worldwide predictions anticipate that approximately 9 million people are going to be affected by 2030 (48).

1.3.1.1 Neuropathology

The neuropathology of PD is characterised by a multi-systemic progressive accumulation of misfolded oligomers and larger aggregates of α–synuclein (α-syn). The extensive distribution of aggregates called Lewy Bodies (LB) leads to a widespread neuronal and synaptic deficit responsible for the subsequent global and progressive derangement of the brain signaling in different portion of the nervous systems (central, peripheral and autonomic) (49). The variability of biochemical changes and the consequences of the described multi-system LB pathology might explain the clinical heterogeneity described in the previous section. According to extensive neuropathological descriptions of PD there are preferential propagation patterns (50, 51). Braak et al described that LB deposition begins to accumulate in the anterior olfactory nucleus, dorsal motor nucleus of the vagus and in the myenteric neurons in the gastrointestinal nervous system (50). After the first occurrence, LB depositions tend to spread trans-synaptically among the nerve cells following a distribution subdivided in 6 stages. According to this model the pathological load throughout the brain progressively increases in a predictable fashion in a caudo-rostral direction reaching in stage 3-4 the mesenchephalon and the dopaminergic system in substantia nigra and the neocortex in the final stages. This staging system presents some caveats since, in many cases, it does not match the quality and progression of the clinical symptoms of PD patients and also the crucial involvement of the substantia nigra and the dopamine system (52,53). The dopaminergic neurons have been conventionally related to motor-symptoms in PD and are considered particularly vulnerable due to the complexity and size of the axonal arborization (54-56). Inclusions of α-syn have been traditionally described in a restricted compartment of the dopaminergic projections (substantia nigra) (57) but recently some authors have suggested a novel pathological hypothesis which claims that the primary neurodegenerative load is in the striatum at the pre-synaptic and axonal levels (58,59). In line with this hypothesis, different research groups (pre-clinical and clinical) have started to observe and examine an early and larger degeneration of dopaminergic axonal terminals rather than substania nigra cell bodies in patients affected by PD (60,61).

1.3.1.2 Dopaminergic markers in PD

The most evident molecular expression of PD is the progressive reduction of dopamine signaling due to the degeneration of dopaminergic striatal projections and substantia nigra cell bodies. The dopamine pathway begins in the liver where the precursor tyrosine is synthesized. Tyrosine is transported into the brain and to the dopamine neurons via diffusion carriers (Figure 5). Tyrosine is the precursor for biosynthesis of dihydroxyphenylalanine (DOPA) by the enzyme tyrosine hydroxylase. DOPA is subsequently converted into dopamine by aromatic aminoacid decarboxylase (AADC) in the dopaminergic neurons. Dopamine is transferred and kept into synaptic vesicles by type 2 vesicular monoamine transporters (VMAT2) until it is released into synaptic cleft to interact at a post-synaptic level with dopamine receptors.

The fate of dopamine in the synapse is modulated with re-uptake mechanisms by the dopamine transporter protein (DAT) which is expressed in the plasma membrane. Dopamine can also be degraded by monoamine oxidase or cathecol O-methyltransferase. Many of the mentioned enzymes have been explored *in vivo* in clinical studies (Figure 5).

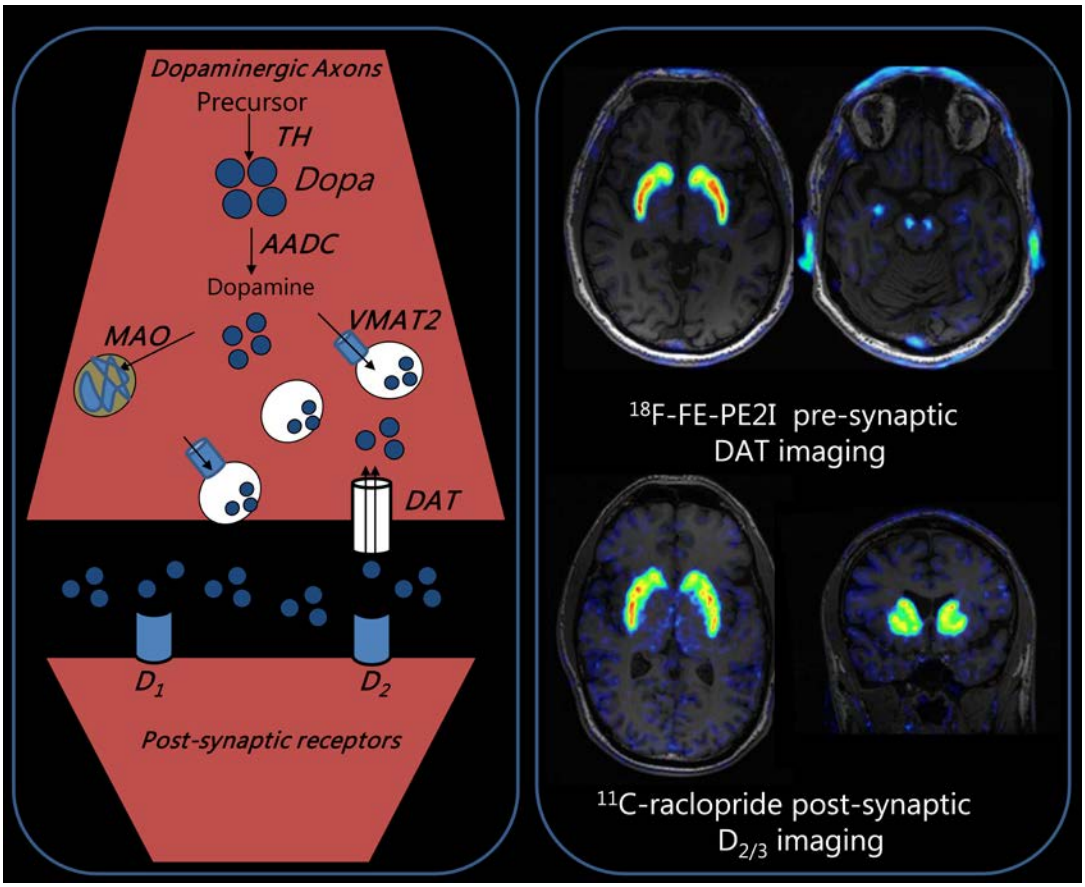

Figure 5. Schematic representation of a dopamine synapse and the relative enzymes and functions (left panel). Representative DAT imaging and $D_{2/3}$ imaging (right panel).

[^{18}F]Fluoro-L-dopa has been used as a biomarker for the dopaminergic functional integrity since it correlates with dopamine cell counts and levels (62) and reflects the activity of the AADC and VMAT2 (DOPA transformation, transport and storage). However, [^{18}F]Fluorodopa uptake might underestimate the extent of the degenerative process in early PD for the presence of compensatory up-regulation (63, 64) and they might be influenced by the effects of the dopaminergic treatment (65).

Targeting VMAT2 is another possibility already employed in clinical setting using the radioligand [^{11}C]DTBZ and more recently an ^{18}F-labeled version [^{18}F]FP-DTBZ (66, 67). VMAT2 imaging has been considered a reliable measurement of dopaminergic integrity (DOPA vesicle storage and release), however the progressive dopamine deficit and therapies may influence the availability of VMAT2 as a consequence of up-regulation mechanisms (68, 69).

DAT imaging (DATscan-SPECT/[^{123}I]FP-CIT) is currently used clinically to support or reject the diagnosis of parkinsonism associated with striatal dopaminergic deficit and for the differential diagnosis with other conditions such as essential tremor, drug-induced/iatrogenic parkinsonism (70-73). Moreover, DATscan imaging enables the identification of another category of patients with parkinsonian-like symptoms without evidence of dopamine depletion in the striatum that are defined as SWEDD (scan without evidence of dopamine deficiency) which have recently generated interesting discussion in the field (74-76). Several PET radioligands have been used to measure the availability of DAT: [^{11}C]β-CFT, [^{18}F]-FP-CIT, [^{11}C]PE2I, [^{11}C]RTI-32 and [^{11}C]methylphenidate among others (77). Although the binding of these radioligands to DAT in PD patients might be influenced by the reduced levels of endogeneous dopamine, DAT binding estimates obtained so far in the striatum with the different probes offer a useful marker of the dopaminergic function impairment.

All pre-synaptic markers (Fluorodopa, VMAT2 and DAT) have been found to decrease with the progression of the disease (78,79). In the early stages of the disease (Mild/stage Hoehn &Yahr 1) the controlateral (opposite to the most affected clinical side) and posterior part of the putamen is the most involved with a reduction estimated to 45-70 % compared to healthy controls (67,68,78,80). Moreover, longitudinal PET studies in different PD cohorts have been able to show that the yearly decline of presynaptic dopaminergic markers in PD pathology is approximately 6-10 % (81-84).

This thesis proposes as presynaptic imaging marker in PD and specifically has the objective to validate a DAT selective radioligand, [^{18}F]FE-PE2I, that has been developed to image the DAT in the striatum and in the substantia nigra (85,86). Dopamine $D_{2/3}$ receptors have also been

examined as post-synaptic markers of the dopaminergic system. Studies employing [^{11}C] raclopride to measure $D_{2/3}$ receptor availabilities have been successfully employed to study post-synaptic differences between PD and the atypical parkinsonisms such as MSA and PSP. Reduced levels of post-synaptic receptors have been found in MSA and PSP compared to PD (87,88). Furthermore PD [^{11}C]raclopride imaging have shown an interesting up-regulation of $D_{2/3}$ receptors in the putamen in early PD drug naïve patients (89) and also in asymptomatic carriers of the Parkin gene mutation (90).

1.3.1.3 Imaging serotoninergic transporter in PD

The involvement of another monoaminergic system (i.e. serotonin) has been also hypothesized in light of the early involvement of the brainstem in the ascending neurodegeneration pattern described by the Braak staging system and in relation to some of the PD non-motor symptoms such as anxiety and depression (91). Supporting this hypothesis different pre-clinical, post-mortem and clinical studies have shown the implication of serotonin system in PD. A seminal post-mortem immuno-histochemistry study strongly suggested an involvement of the different serotonin containing nuclei of the raphe in the brainstem (dorsal, medial and caudal) in PD patients (92). Another post-mortem study has demonstrated that both the neurotransmitter serotonin (5-HT) and its transporter (5-HTT) were reduced by 30 to 66%, with a preferential involvement of the caudate, compared to the putamen (93). Moreover, studies with PD animal models were able to describe that in presence of a dopaminergic dysfunction, the conversion of L-dopa to dopamine might be carried out by serotoninergic projections innervating the striatum (94). PET studies in PD have shown approximately a 30% decrease of 5-HTT availability in the subcortical and cortical areas (95, 96). More recently, higher 5-HTT availability in the dorsal raphe nuclei and limbic regions has also been found in PD patients with higher scores of depression (97, 98). These studies suggest that 5-HTT availability is already decreased in early PD patients, it is inversely related to disease stage (95) and positively related to scores of depression (97-99). Of interest is that the serotonin system seems to be involved in the pathophysiology of levodopa induced dyskinesia.

The capability to evaluate serotoninergic targets in the different raphe nuclei has so far been challenged by the limited resolution of the PET system for such small brainstem structures. In this thesis, high-resolution PET imaging and a specific methodology to measure the 5-HT availability in the different nuclei of the brainstem have been used. The method developed can be used to examine the 5-HTT in the brainstem of PD patients.

1.3.2 Huntington's disease

Huntington's disease is a genetically determined neurodegenerative disorder characterized by a highly variable and complex clinical phenotype consisting of movement disorder, neuro-psychiatric impairments and cognitive deficits. Motor deficits are characterized by choreic movements, dystonia, parkinsonism, oculomotor dysfunctions, gait and balance disturbances, dysarthria and dysphagia. Cognitive symptoms encompass deficits in the executive dysfunction (concentration, attention, multi-tasking), lack of motivation and insight, reduction of problem solving and social cognition. Psychiatric problems include depression, anxiety, obsessive-compulsive disorders, irritability, disinhibition, delusions, apathy and suicidality (100). HD belongs to the family of expanded CAG repeat disorders and is considered a progressive neurodegenerative disorder. The gene responsible for HD (IT15) was identified in 1993 (101, 102). It is also defined as the *huntingtin* gene for the protein product that is coded by the gene. Different studies showed prevalence estimates of 5-10 patients per 100.000 in Europe, the two Americas and Australia and lower estimates in Finland and Asia (103, 104). Prevalence estimates are likely to be underestimated worldwide. The disease becomes clearly evident between 30 and 55 years. The age of onset is predictable but also influenced by other genes beside the HD gene and by environmental factors (105-107). The availability of genetic tests made it possible to identify HD gene expansion carriers (HDGECs) before their evident clinical onset. The disease can thus be described in two different periods: the "pre-manifest" and the "manifest" period. When it is "manifest" the progression is inevitable and quite rapid (15-20 years) even if the natural history may vary (108). The dysfunctions associated with the presence of mutant huntingtin (mHTT) are of complex nature and not yet fully understood. The molecular pathogenicity of mHTT seems to be connected to a typical conformational change and to its tendency to form insoluble aggregates in different neural cells. The specific cellular mechanisms involved in the neurodegenerative process are not yet fully understood, but a toxic gain of function is suspected (109, 110). From a research and translational perspective, HD represents a unique suitable human model of neurodegeneration, since it is by nature monogenic, and it is associated with a long prodromal phase with a well characterized clinical evolution.

1.3.2.1 Neuropathology

The variability and richness of clinical signs in different domains are the consequence of a broad deranged signaling mainly linked to the loss of functions and degeneration of the cortico-striatal connections, the toxic gain of function of mHTT and to a toxic accumulation of protein

aggregates. As with other neurodegenerative diseases, the pathological process in HD begins several years before the evident clinical manifestation. MSNs in the striatum have been traditionally considered the main target of degeneration occurring in HD. The traditional neuropathological grading system was developed according to the neurodegenerative pathological (gross and microscopic level) temporal patterns found in the striatum. This system has five grades of severity of striatal involvement (111). Post-mortem autoradiographic studies of patients with HD at different stages have also suggested specific patterns of molecular degeneration based on the specific neurochemistry of the basal ganglia circuitry (112). Interestingly, the $GABA_A$, cannabinoid CB_1, dopamine D_2 and adenosine A2a receptor density seems to be involved and decreased in early neuropathological grades of HD in the striatum whereas an increase of GABA-A receptors in globus pallidus pars externa (GPe) has been observed. The latter has been interpreted as a compensatory regulation of pallidal receptors in response to the ongoing denervation (113). Nowadays, MSNs are considered no more than one of the vulnerable neuronal populations. It is becoming more evident that the disease has a more multisystem character (114) with evidences of structural and functional abnormalities in the cerebral neo-and allocortex, selected thalamus nuclei, pallidum and different nuclei of the brainstem such as the substantia nigra, the pontine nuclei, reticulotegmental nucleus of the pons, superior and inferior olives (115, 116).

1.3.2.2 Dopaminergic Imaging markers in HD

Since the major pathological features in HD were traditionally related to the loss of MSNs in the striatum, different *in vivo* PET studies have been mainly focused on post-synaptic dopaminergic receptors. Reduction of dopamine D_1 and D_2 receptor availability were reported both in manifest and pre-manifest HDGECs.

Multi receptors PET studies examining D_1 receptors with [^{11}C]SCH23390 and D_2 receptors with [^{11}C]raclopride showed similar impairments of the two receptor systems in manifest (117, 118) and pre-manifest (119) HDGECs. Different PET studies performed with [^{11}C]raclopride showed approximately 40-60 % loss of $D_{2/3}$ receptors in the striatum of manifest HDGECs and approximately 10-50 % reduction in heterogeneous and small groups of pre-manifest HDGECs (117, 120-123) as compared to healthy control subjects. The variability, between studies, regarding the reduction of $D_{2/3}$ receptors found in pre-manifest HDGECs might represent the consequence of a broad range of CAG repeats and the burden of pathology among the HDGECs examined. Conflicting results have also been obtained when dopamine $D_{2/3}$ receptors availability was measured in extra-striatal areas (123-125).

Interestingly, the involvement of the post-synaptic system ($D_{2/3}$) has been coupled with increased levels of microglial activation (126, 127).
In vivo PET studies with pre-synaptic markers are limited. Reduction of striatal VMAT2 binding have been reported in manifest HDGECs with the radioligand [^{11}C]dihydrotetrabenazine with a more severe involvement in patients with the akinetic-rigid motor phenotype compared to the choreiform one. The estimated reduction of 25 % compared to healthy controls was estimated with partial volume effect correction (128). In addition, in a small group of manifest HDGECs, 50 % reduction of DAT binding was described with [^{11}C]beta-CIT-PET (117).

1.3.2.3 Imaging phosphodiesterase 10 A in HD

Among many interesting striatal targets, the intracellular Phosphodiesterase 10A (PDE10A) enzyme has recently gained a scientific attention for the key role in the regulation of striatal signaling and for the presence of suitable pharmaceutical compounds able to modulate it. PDE10A is highly expressed in MSNs of the striatum, at the confluence of the corticostriatal glutamatergic and the midbrain dopaminergic pathways, where it encodes the hydrolysis of both cyclic adenosine monophosphate (cAMP) and cyclic guanosine monophosphate (cGMP) (129). The resulting signaling cascades are likely to modulate the molecular signalling in the corticostriatothalamic circuit. *In vivo* imaging of PDE10A has been proposed as a suitable biomarker for the study of molecular changes in the striatal MSNs. Recent PET imaging studies investigating the availability of PDE10A in HDGECs suggested a specific alteration of this protein along with the neurodegenerative process. There are several radioligands currently validated and used *in vivo* in clinical PET studies: [^{18}F]JNJ42259152 (130), [^{18}F]MNI-659 (131, 132), [^{11}C]IMA107 (133) and [^{11}C]Lu AE92686 (134). Several studies have already been performed in manifest and pre-manifest HDGECs with the aim of examining the PDE10A enzyme. The work of Ahmad et al (130) was the first study showing a dramatic reduction (after PVE correction) of the enzyme in five manifest HDGECs compared to eleven non age matched healthy controls (70% in the caudate and 65% in the putamen). In the first cross sectional study employing a fully validated PDE10 radioligand [^{18}F]MNI-659 (139), Russell et al showed an average reduction of PDE10A availability of 50% in three pre-manifest and eight manifest HDGECs compared to age-matched healthy controls (131). The same group has recently published a longitudinal study in which eight HDGECs (6 manifest and 2 pre-manifest) underwent two [^{18}F]MNI-659 PET measurements one year apart. On average, the estimates of annual PDE10A loss was 16.6% in the caudate, 6.9% in the putamen and 5.8% in the globus

pallidus (132). The outcome measures of this study were not corrected for PVE. More recently, using [^{11}C]IMA107 PET, a group of twelve early pre-manifest HDGECs (approximately 25 years before the predicted onset) showed respectively 25 and 33% reductions in the striatum and in the globus pallidus compared with age-matched healthy controls. At that "stage" in HDGECs, no evident volumetric changes were detected in the grey and white matter structures as result of a morphometric analysis (133).

So far, the above mentioned studies have been focused only on the examination of the PDE10A enzyme, but have not examined how the loss of PDE10A is related to the loss of $D_{2/3}$ receptors, a well-established striatal marker in HD. In addition, those PET studies have examined PDE10A only in some stages of the disease, but data across a wider range of disease, including both pre-manifest and manifest stages are lacking. In this thesis, PDE10A has been examined in relation to $D_{2/3}$ receptors in HDGECs studied at different stages of the disease.

2 AIMS

In this research plan, the overall aim was to utilize state-of-the-art molecular imaging with PET to evaluate *in vivo* molecular targets that might be useful to examine early changes in PD and HD patients.

In **paper I,** we have been focused on examining the suitability of [^{18}F]FE-PE2I as a tool for imaging the nigrostriatal pathway in PD.

In **paper II,** the aim was to develop and validate a user independent approach tailored for the brainstem to quantify 5-HTT availability with [^{11}C]MADAM, with the intention to apply the method in a cross sectional study examining early PD patients.

In **paper III,** we wanted to apply the knowledge gained in the previous two studies to quantify *in vivo* the DAT availability in the substantia nigra, axons and striatal terminals in a larger cohort of early PD patients using [^{18}F]FE-PE2I with a tailored template-based approach.

In **paper IV,** we wanted to study the patterns of age related changes of two basal ganglia molecular targets (phosphodiesterase 10A and $D_{2/3}$ receptors) in healthy volunteers in relation to structural changes.

In **paper V,** the aim was to evaluate the availability of the phosphodiesterase 10A enzyme in basal ganglia across a broad disease spectrum of HDGECs (i.e., early pre-manifest, late pre-manifest, stage 1, stage 2).

3 METHODOLOGICAL CONSIDERATION

Materials and methods used in the present thesis are comprehensively described in each respective article or manuscript. In the following section some of the general and specific methodological aspects are presented and discussed.

3.1 POSITRON EMISSION TOMOGRAPHY

The PET measurements were performed using the High Resolution Research Tomograph (HRRT). The HRRT is a high resolution PET system (Siemens Molecular Imaging) designed for human brain and small animal imaging. The system consists of eight panel detectors with an octagonal array, which have two layers of Lutetium Oxyorthosilicate (LSO) (2.4 x 2.4 x 10) and LYSO crystals, a total number of crystals of 59,904 x 2 layers, an axial field of view of 24 cm, collecting 207 planes in the reconstructed images, with a slice thickness of 1.218 mm, and an average resolution of 2.3 mm full-width half-maximum (FWHM) in all directions. The resolution has been further improved by modeling the point spread function (i.e. the resolution of the system) in the reconstruction algorithm (Ordinary Poisson (OP)-3D-ordered subset expectation maximization (OSEM)) (135).

3.2 MAGNETIC RESONANCE IMAGING

MR examinations were acquired for several purposes:

a. to rule out pathology or vascular changes.
b. to obtain anatomical images for coregistration with PET images
c. to define volumes of interest
d. to retrieve normalization parameters to the standard space

MRI images are generally coregistered to PET and segmented into gray matter (GM), white matter (WM), and cerebrospinal fluid (CSF) using SPM5 (Wellcome Department of Cognitive Neurology, University College London) of Freesurfer. MRI examinations of six subjects in paper II were collected with a 1.5-Tesla GE Signa Excite MR system (3DSPGR; 156 slices of 1 mm thickness, FoV = 256 mm, matrix = 256 Å~ 256, resolution = 1 Å~ 1 Å~ 1 mm, TE = 5 ms, TR = 20 ms). The rest of MR images for the subjects recruited for the study presented in paper I-II-III have been acquired with a GE MR750 3-Tesla system (IR-SPGR; 32 channel

coil, 176 slices of 1 mm thickness, FoV = 256 mm, matrix = 256×256, resolution = 1×1×1 mm, TI = 450 ms, TE = 3.18, TR = 8.16). MR images for the subjects recruited for the study presented in paper IV-V were collected with a GE MR750 3 Tesla system (IR-SPGR; 8 channel coil, 176 slices of 1 mm thickness, FoV=256 mm, matrix 256×256, Resolution 1×1×1 mm. TI=450 ms, TE=3.18, TR =8.16).

3.3 IN VITRO AUTORADIOGRAPHY STUDIES

Autoradiography is an in vitro technique used to produce high-resolution images of the 2D distribution of a radioactive substance. In relation to PET studies the autoradiography technique might be helpful to verify or validate a given molecular target of interest (i.e. histochemical validation of in vivo imaging target) or to obtain detailed maps of receptor/transporter/enzyme distribution (i.e. whole hemisphere autoradiography). The principle of in vitro autoradiography studies is to incubate tissue sections with a radiolabelled compound and to measure the concentration of radioactivity in the tissue using a phosphoimager. In our setting, autoradiography studies were carried out essentially as described earlier in previous publications (136). In brief, post mortem whole hemispheres were removed, frozen, and cryosectioned into 100 µm-thick coronal sections using a heavy-duty cryomicrotome. For the examination conducted in paper II sagittal and axial section of the brainstem were used. In the experiment all sections were incubated at room temperature with the radioligand for the serotonin transporter [^{3}H]MADAM (137). Specific binding was measured after blocking with a selective 5-HTT inhibitor (fluoxetine).

3.4 KINETIC MODELING AND OUTCOME MEASURES

In paper I, all the PET studies were analyzed with the simplified reference tissue model (SRTM) and the Logan graphical analysis, using the cerebellum as reference region and the software PMOD. As result of the kinetic models, estimates of regional binding potential relative to the non-displaceable compartment (BP_{ND}) were selected as the study outcome measure.

In paper I, II and III, parametric images of BP_{ND} (voxel-based maps) were obtained with the software WAPI, using Logan graphical analysis and the cerebellum as a reference region.

In paper 4 and 5, the kinetic model of choice to estimate the outcome measure for [^{18}F]MNI-659 was the two-tissue compartment model (2TCM) including the arterial input function. This model was used to derive indirectly BP_{ND} (V_T-V_{ND}/1). V_T represents the total distribution volume in the

target regions (striatum and globus pallidus) and V_{ND} represents distribution volume in the non-displaceable compartment. The choice of 2TCM was based on a preliminary evaluation performed in 15 healthy subjects. One-Tissue compartment model (1TCM) and SRTM were not optimal in describing the time activity curves of [^{18}F]MNI-659 because of a number of fitting failures or poor model fits. 2TCM was the method that consistently generated a better fitting for all the ROIs except for the cerebellum, in all subjects. A straightforward solution to compensate the fitting imprecision in the cerebellum was to include the fraction of the blood volume as a fifth parameter. Visual inspection of parametric images of [^{18}F]MNI-659 provided evidence of high binding of the radioligand in the venous sinuses in the brain. PDE10A is present in vascular smooth muscle cells (138). Therefore, the binding observed in the venous sinuses could be related to the presence of PDE10A in the vasculature. In a low binding region as the cerebellum, the vascular binding of [^{18}F]MNI-659 is not negligible and might contribute to the signal measured in this region. The discrepancies observed in the performance of SRTM compared to the already published studies with [^{18}F]MNI-659 (131,132, 139) might be related to different PET system employed in those studies. Differences in the sensitivity to low counting statistics of the HRRT PET system may have influenced the reported differences in fitting performance in the cerebellum. In paper IV-V, the kinetic model of choice to retrieve the outcome measure BP_{ND} for [^{11}C]-raclopride was SRTM.

3.5 PARTIAL VOLUME EFFECT AND CORRECTION

In paper IV and V, the outcome measures presented were obtained from regional time-activity curves corrected for Partial Volume Effect (PVE). PVE is an phenomenon related to the limited resolution of the PET system (140). Because of PVE, the radioactivity concentration in different regions is under or over estimated due to “spill-over” of measured radioactivity between neighboring regions. This effect is more evident when the contours of the regions of interest are delimited by other regions or tissues with different target availability such as it is present in the basal ganglia. This effect is also enhanced by the presence of significant brain atrophy resulting in a predictable underestimation of target availiability (i.e. striatal atrophy in the striatum in HD). The application of PVE correction (PVEc) methods is thus important, despite the fact that such methods can be associated with possible biases due to noise amplification. Limitations related to the intrinsic presence of tissue in-homogeneities and susceptibility to suboptimal MRI and PET preprocessing (segmentation and co-registration) (141) should also be considered. The PVEc method used in paper IV and V is an implementation of the Rousset method that is based on the estimation of a geometric transfer

matrix (GTM) to describe and thus correct for signal contamination occurring between neighboring ROIs.

The actual implementation in our setting includes the effective resolution and point spread function of the HRRT PET system and the anatomical details and precisions of the ROIs boundaries provided by the MRI preprocessing with Freesurfer. The use of high resolution PET imaging and the application of PVEc to the PET data acquired in this thesis were aimed to achieve high accuracy of the quantification of molecular target in the striatum and small brain regions (135) (Figure 6).

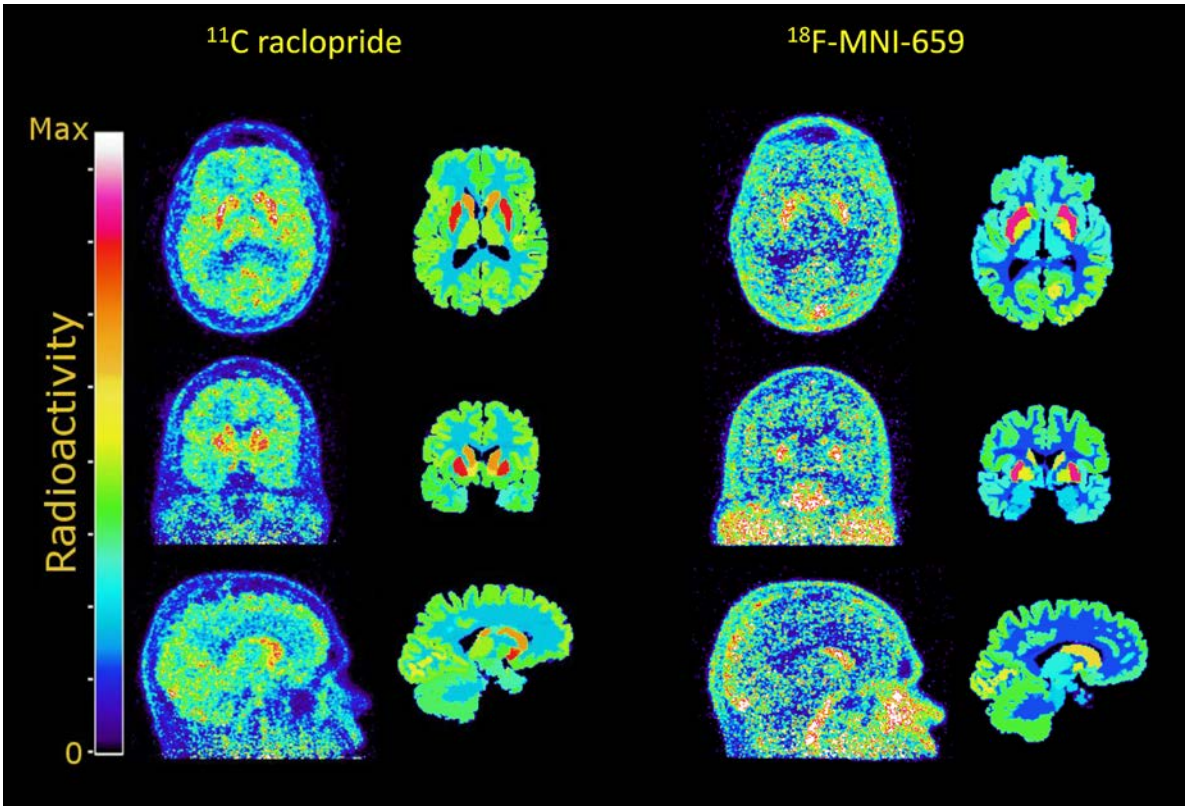

Figure 6: Representative average [^{18}F]MNI-659 (left) and [^{11}C]raclopride (right) images before and after partial volume correction (PVEc). Courtesy of Martin Schain.

3.6 TAILORED TEMPLATE-BASED ANALYSIS USING PARAMETRIC IMAGES

In paper II and III, 3T-MR images and HRRT-PET parametric images were used to generate a template of [^{11}C]MADAM and [^{18}F]FE-PE2I binding to 5-HTT and DAT. An automated brainstem weighted co-registration method developed for fMRI imaging analysis (142) was used to obtain an accurate normalization of individual structural 3T-MR images and HRRT-PET parametric images into the standard Montreal Neurologic Institute (MNI) space. The normalization was performed with a two-step approach based on two consecutive affine linear transformations applied on the individual T1-weighted MRI scans using FLIRT, a linear Image

Registration Tool from FMRIB's Software Library (FSL, Oxford) (143). An extended MNI-152 brainstem mask that included the third ventricle, part of lateral ventricle and part of the thalamus was used as a reference volume, to weigh the second full affine transformation. The parameters obtained with the concatenation of the two transformations were subsequently applied to ten individual parametric PET image (after co-registration to MR space) to create a set of ten parametric images in the MNI standard space. Those ten parametric images (all in the standard MNI space) were subsequently averaged in order to obtain a representative PET template of 5-HTT and DAT binding (Figure 7). Normalization parameters were obtained also from subjects not involved in the generation of the template.

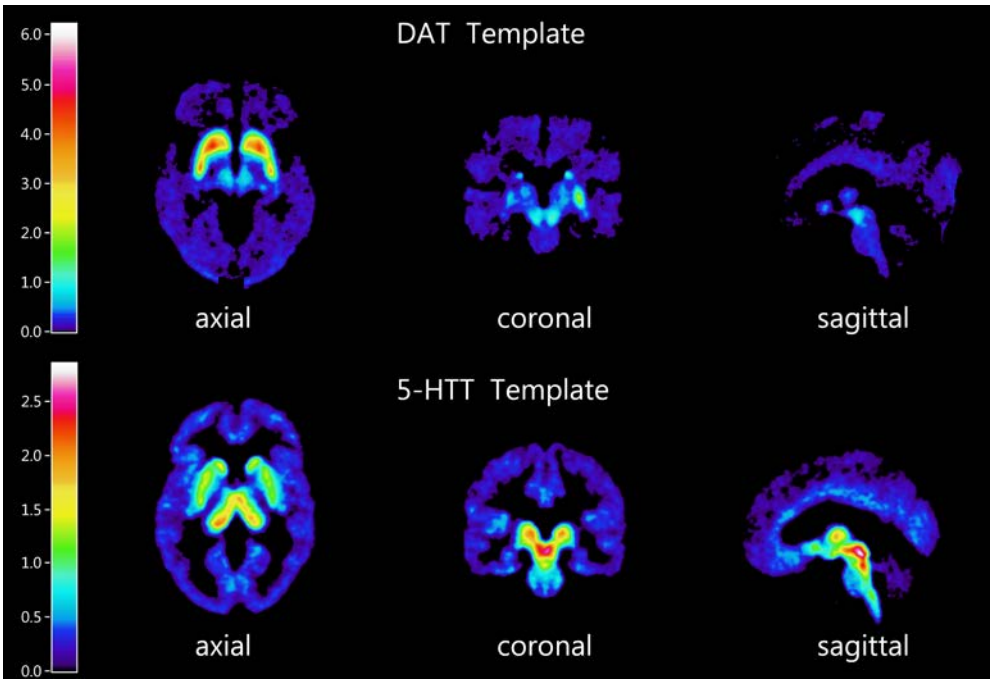

Figure 7. Images of the two PET templates for 5-HTT and DAT. Axial, coronal and sagittal. Color bars specify Binding potential (BP_{ND}) values of the brain PET images.

In Paper II, template-based volumes of interest (VOIs) were defined on the PET template using a previously published threshold-based VOI-delineation method (26). In short, the delineation of each VOI was initiated with the definition of a bounding box that enclosed the anatomical structure in the co-registered MR images. The bounding box was then reduced, so that only voxels displaying higher BP_{ND} values than a threshold were included in the final VOI. The threshold used for the erosion of the bounding box was set to include the relevant binding in each brain region and to provide volumes of each anatomical structure in agreement with those found in the literature (26).

The VOIs generated on the PET template included the ventral midbrain, superior colliculi, dorsal raphe, median raphe and the caudal raphe.

In Paper III, VOIs were manually delineated on the DAT template using anatomical and DAT binding patterns by overlaying the two modalities (MR-MNI template and HRes DAT template) using the Human Brain Atlas software. The VOIs generated on the PET template included the caudate, putamen, ventral striatum and substantia nigra. Noteworthy the template enabled the visualization of DAT binding of [^{18}F]FE-PE2I along different axonal projections generated from the substantia nigra. For both papers II and III, all template-based VOIs were then transformed and projected to the individual space (using the inverted normalization parameters) and applied upon each subject's parametric image to estimate the average regional BP_{ND} values.

3.7 RECRUITMENT AND CHARACTERISTICS OF PARKINSON AND HUNTINGTON'S DISEASE PATIENTS

In paper I and III PD patients were recruited at the movement disorders clinic of the Karolinska University Hospital in Huddinge and through the Swedish Parkinson patient association in Stockholm (Parkinsonförbundet). Patients satisfied the clinical diagnosis of PD according to the U.K. Parkinson Disease Society brain bank criteria (57). Patients were evaluated while in "on" state with the Hoehn and Yahr (H&Y) staging and using the motor part of the Unified Parkinson's Disease Rating Scale (UPDRS-m) (**Table 1**).

PD patients	Gender	Age	Education	MMSE	Disease Duration	UPDRS motor	Hoehn & Yahr	Side	LEDs
P01	M	64	10	28	12	23	2	Left	736
P02	M	74	10	28	0.5	11	1	Right	De Novo
P03	F	66	10	30	6	18	2	Right	940
P04	M	47	12	27	4	21	1.5	Right	240
P05	M	68	16.5	30	0.25	18	1	Left	De Novo
P06	M	52	12	29	0.25	8	1	Right	160
P07	M	46	16.5	30	0.6	16	1	Right	160
P08	M	67	16	28	2	30	1.5	Right	160
P09	M	60	15	28	1.5	27	1.5	Right	322
P10	M	58	22	29	4	17	1	Left	342
P11	M	70	18	29	2	20	1	Right	60
P12	M	58	16	30	3	20	1.5	Left	798
P13	F	70	12	28	3	27	1.5	Right	100
P14	M	71	18	30	2.5	26	2	Left	400
P15	M	52	19	30	2	25	1.5	Right	241
P16	M	65	13	27	2.5	18	2	Right	400
P17	M	67	15	28	3.5	25	2	Left	559
P18	F	67	15	29	2	24	1	Right	100
P19	F	65	18	27	3	18	1	Left	300
P20	F	65	15	29	2	31	2	Right	300
Average±SD		**62±8**	**15±3**	**28.7±1**	**2.8±2**	**20.9±5.9**	**1.4±0.4**		351±253

Table 1. Demographic and clinical data of Parkinson´s patients. Key: MMSE, Mini-Mental State Examination; F, female; M, male; UPDRS, Unified Parkinson's Disease Rating Scale; Side, the clinical most affected side; LED; Levo-Dopa Equivalents. The first ten PD patients were included also in paper I. All PET measurements were performed in "off" state.

In paper V, HDGECs were also participating to REGISTRY or ENROLL-HD studies and were pre screened for possible eligibility. HDGECs were recruited and screened in six clinical sites in Sweden, Denmark, Norway and the Netherlands.

The stratification of HDGECs was based on the number of CAG repeats, age of the subject and by specific clinical outcome measures generated with validated clinical assessments tools such as the Total Functional Capacity (TFC) score and Total Motor Score of the Unified Huntington's Disease Rating Scale (UHDRS) (144). The functional section of the UHDRS (TFC) provides an assessment of HDGECs manifest patients at a functional level and it codifies patients in five stages. Different functionalities are evaluated in the domains of workplace, finances, domestic chores, activities of daily living and requirements for unskilled or skilled care. The motor section of the UHDRS (TMS) is a clinical rating scale that evaluates manifest HDGECs in the motor domain (i.e. eye movements, amount of chorea/dystonia/bradykinesia/dysartria, gait and balance).

REGISTRY and ENROLL-HD are studies collecting prospective data on the phenotypical characteristics of HDGECs and individuals that are part of an HD family.

In paper V HDGECs were subdivided in different stages of the disease (early pre-manifest, early pre-manifest, stage 1 and stage 2) (**Table 2**).

HDGECs	Early Premanifest	Late Premanifest	Stage I	Stage II
Number	**10**	**15**	**15**	**5**
Gender	**3M/7F**	**6M/9F**	**11M/4F**	**2M/3F**
Age	**39.2±7.1**	**39.4±6.6**	**50.2±10.2**	**56.4±14.3**
CAG	**41.3±1.1**	**44.5±1.5**	**43.8±2.4**	**43.6±5.5**
DBS	**222.6±30.3**	**338.4±51.8**	**397.3±58.2**	**398.4±133.6**
TMS	**0.3±0.7**	**0.8.±1.0**	**25.6±9.4**	**31.6±7.1**
TFC	**13±0.0**	**12.7±0.7**	**11.9±0.6**	**8.6±0.9**

Table 2. Clinical characteristics of Huntington Disease Gene Expansion Carriers (HDGECs) in the different stages. Key: F, female; M, male; DBS, Disease burden score: age × (CAG length–35·5); mUHDRS-TMS, unified Huntington's disease rating scales- total motor score.

4 RESULTS AND REFLECTIONS

4.1 PAPER I

4.1.1 Evaluation of [^{18}F]FE-PE2I as radioligand for DAT imaging *in vivo* in PD patients and in healthy controls.

The study included 10 early PD patients (9M/1F, 60±9y, Hoehn&Yahr: 1-2; Unified Parkinson's Disease Rating Scale motor: 18.9±6.7) and 10 controls (9M/1F, 60±7y). Regions of interest for caudate, putamen, ventral striatum, substantia nigra and cerebellum were drawn on co-registered magnetic resonance images. The outcome measures was the binding potential (BP_{ND}) estimated with the simplified reference tissue model (SRTM) and the Logan graphical analysis (LoganRef), using the cerebellum as reference region. Time stability of BP_{ND} was examined to define the shortest acquisition protocol for quantitative studies. The wavelet-aided parametric imaging method was used to obtain high-resolution BP_{ND} images. Venous blood was drawn to compare protein binding, parent fraction and radiometabolite composition in PD patients and healthy controls. The results showed that [^{18}F]FE-PE2I has a similar metabolism in PD patients and control subjects and that cerebellum is a suitable reference region. Accurate quantification could be achieved using 66 minutes of PET data. DAT availability in PD patients was significantly lower than in controls, by 69% in the putamen, 31% in the caudate, 32 % in the ventral striatum and 33% in the substantia nigra. These findings suggested that [^{18}F]FE-PE2I is a suitable radioligand for DAT quantification in both striatum and substantia nigra in PD patients. The quantification can be performed non-invasively using the cerebellum as reference region. The suitable kinetic properties permit also to use simplified acquisition protocols.

4.1.1.1 Reflections

The suitability of [^{18}F]FE-PE2I as an imaging tool to reliably measure DAT availability in striatal and extrastriatal regions in PD patients was based on the following considerations partly from previous studies (85, 145, 146) (a-b-c-d) and from the results obtained with this study (d-e-f-g):

a. [^{18}F]FE-PE2I is labelled with ^{18}F, therefore the radioligand could be used even in imaging facilities without a cyclotron and a radiochemistry unit.

b. [^{18}F]FE-PE2I has adequate affinity (Ki=12 nM) and selectivity for the DAT (>80-fold higher affinity to DAT than to 5-HTT). These properties enable to image the DAT also in the substantia nigra.
c. Peak equilibrium of [^{18}F]FE-PE2I in the striatum and the substantia nigra is reached between 20 and 40 min, assuring accurate quantification of DAT in both regions.
d. Cerebellum is a suitable reference region, enabling the quantification in a non-invasive way.
e. The fraction of parent and radiolabelled metabolites of [^{18}F]FE-PE2I did not differ significantly between PD patients and controls. The fraction of the radiolabelled metabolite of [^{18}F]FE-PE2I that might enter the brain (hydroxy-methyl analog) was negligible (<2%) and should not affect the quantification. There is therefore no need to collect blood samples and perform metabolite analysis in future PET studies.
f. The accuracy of quantification can be achieved using ~66 minutes of PET measurements in the caudate, putamen, ventral striatum and substantia nigra.
g. [^{18}F]FE-PE2I can be analysed with non-invasive and simplified imaging protocols for clinical studies in PD studies.

From a clinical perspective the possibility to study with the same radioligand the availability of DAT at pre-synaptic level (striatal terminals) and where the dopaminergic projections are generated (cell bodies of dopaminergic neuron in the substantia nigra) represent a unique opportunity for future application in clinical studies of PD and atypical parkinsonisms (see section **5.1.1.1**).

From a learning perspective this study gave me the opportunity to understand the principles of PET data analysis and kinetic modeling. The challenges of this study introduced me to the complexity of the essential infrastructure and expertise needed for the collection and gathering of all relevant data (i.e. clinical outcome measures). A considered amount of time was spent to adjust and adapt the methodological skills connected to the study program and to the acquisition and quantification of PET data. I'm grateful to have had the opportunity to work with [^{18}F]FE-PE2I which is a radioligand with optimal image and kinetic properties. These results have been achieved after approximately 10 years of progressive validation and development.

4.2 PAPER II

4.2.1 Quantification of 5-HTT binding in small nuclei of the brainstem: a validation of a template based approach.

The template-based analysis was performed on 16 healthy subjects (14M/2F, 21-67 y) that were examined with [^{11}C]MADAM using the HRRT system. Individual BP_{ND} parametric images of 5-HTT availability were generated for each subject. VOIs were defined with a template-based method described in the previous section and then transformed and applied to each subject's parametric image to estimate regional BP_{ND} values. The VOIs of this study were the ventral midbrain, superior colliculi and the dorsal-median-caudal raphe. To validate this user-independent approach, regional template-based BP_{ND} values were compared to subject-based BP_{ND} values obtained using a threshold-based ROI-delineation method at individual level (23) and with the specific binding obtained with post-mortem autoradiography studies with [^{3}H]MADAM in sections that included the above mentioned regions.

The distribution of template-based BP_{ND} values was consistent with the pattern of specific binding previously obtained from previous post-mortem autoradiography for all subjects with a relative order of BP_{ND} as follows: dorsal raphe > median raphe > superior colliculi > ventral midbrain > caudal raphe (Figure 8).

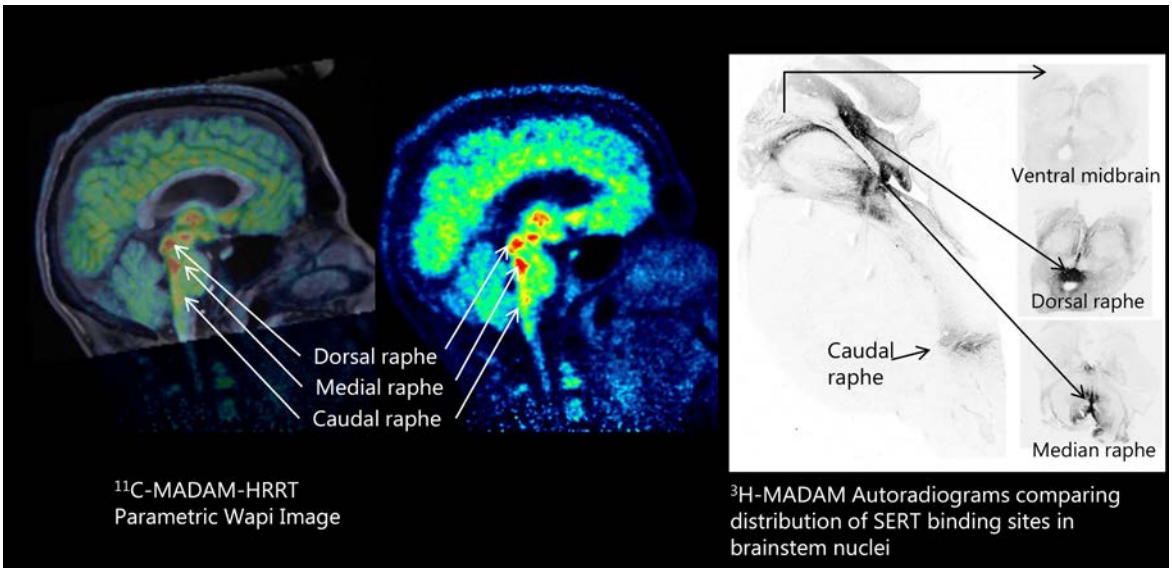

Figure 8. Distribution of SERT binding sites in brainstem nuclei: PET and post mortem autoradiography findings (left and right panel). Sagittal plane sections of 5-HTT distribution patterns obtained with PET (representative parametric images) with [^{11}C]MADAM and with autoradiography studies with [^{3}H]MADAM.

The values obtained with the template based approach were systematically lower than those obtained using individually defined ROIs, although a significant correlation between BP_{ND} obtained with the two methods was observed (r^2=0.83). *In vitro* post-mortem distribution of [^{3}H]MADAM measured with autoradiography confirmed high specific binding in the dorsal and median raphe followed by superior collicoli and caudal raphe and intermediate values in the ventral midbrain striatum and amygdala. There was a relationship (r^2=0.62) with the template-based BP_{ND} in the comparable regions.

4.2.1.1 Reflections

The proposed template-based method together with the high resolution PET imaging represent a relevant development for the quantification of 5-HTT in the brainstem nuclei. Indeed, to the best of our knowledge, literature data for the entire set of VOIs quantified in this study are not available except for the dorsal raphe. The current golden standard for the definition of brain stem regions (i.e. dorsal raphe) is the manual definition of the region on MRI images. This approach has inherent difficulties that might lead to an erroneous definition and localisation of the structures (147). The method proposed in this study provides a more robust quantification of the 5-HTT in the brainstem. The possibility to quantify the different portions of the raphe nuclei (dorsal-median-and caudal) is relevant for the study of the neurobiology of the serotonin system (148). There are indeed several CNS-disorders in which serotonin neurons in the brainstem might be affected. In this respect, the greatest benefit of using a template-based approach for definition of VOIs is that the assumption regarding the volume of the structure is only introduced at a group level. The template-based approach is thereby less prone to suboptimal sampling attributable to the highly variable brainstem anatomy in term of dimensions and orientation, to the intrinsic variability in the localisation of the raphe nuclei complex and to changes of 5-HTT availability due to aging processes or neuropathological modifications.

From a learning perspective this paper helped me in the development of skills related to the analysis of PET data in a less conventional way. In that respect, it was the first experience with generation of a functional template for PET analysis. This study allowed me to deep the understanding of the anatomy and functions of small monoaminergic nuclei enriched in the brainstem and their relevance in studying CNS disorders in which an involvement of those structures it has been already established. On the other hand, it made me aware of the actual difficulties and challenges of the neuroimaging communities in studying, in vivo,

some of the presented brainstem structures. This study introduced me to the use of post-mortem autoradiography studies that turned to be important in the development of competences and knowledge that are gained by the comparisons between in vitro post-mortem applications and in vivo PET studies.

4.3 PAPER III

4.3.1 DAT availability in the substantia nigra, axons and striatal terminals in early PD patients

As reported in **study 1,** [^{18}F]FE-PE2I is a radioligand with image properties that enables the visualization and the reliable quantification of DAT availability also in the substantia nigra. By generating a DAT template as described in the section **3.6** we were able to clearly visualize the presence of binding located even along efferent fibers from the substantia nigra (Figure 10). Template-based ROIs were anatomically delineated (manually) on striatal (caudate, putamen and ventral striatum) and extrastriatal (substantia nigra) regions and along nigro-striatal (NST), nigro-pallidal (NPT), nigro-thalamic tracts (NTT).

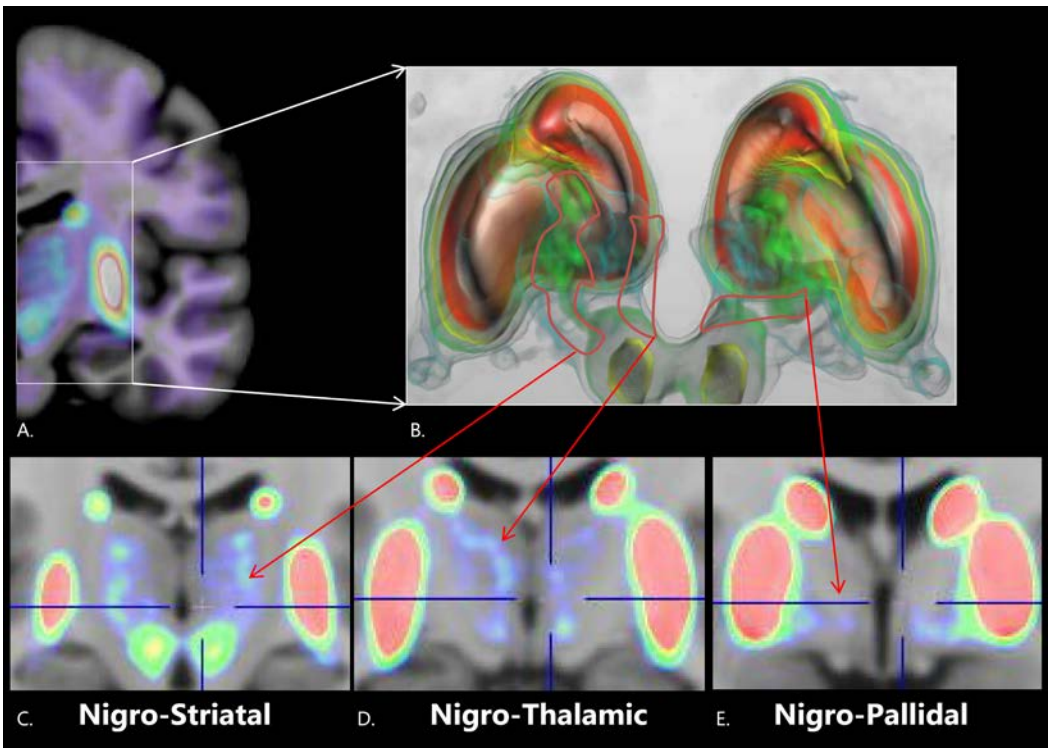

Figure 10. Anatomical study of DAT binding in dopaminergic axonal projections. **A.** Coronal section, at striatal level, of DAT template overlaid on MRI MNI template. **B.** Striatal 3D rendering obtained from DAT template of [^{18}F]FE-PE2I. **C-D-E**. Coronal sections at mesencephalic and dienchephalic level displaying the DAT binding in different dopaminergic projections.

With the presented methodology it became feasible to image the DAT availability in the entire dopaminergic nigro-striatal system and apply this analysis to PD patients. In early PD patients we found significantly lower BP_{ND} values compared to healthy controls in the putamen (PD: 1.33±0.7 vs HC: 4.40±0.6), caudate (PD: 2.42±0.8 vs HC: 4.03±0.6), ventral striatum (PD: 2.21±0.7 vs HC: 3.45±0.7) and substantia nigra (PD: 0.58±0.1 vs HC: 0.84±0.1) (p<0.001). Average BP_{ND} values in the tracts were much lower than in the substantia nigra without a significant difference between the two groups (PD: 0.42±0.1, HC: 0.47±0.1). The largest differences in DAT availability in the tracts between PD patients and healthy controls were found in the nigro-pallidal tract (PD: 0.32±0.1, HC: 0.44±0.1).

This difference did not reach statistical significance after Bonferroni´s correction (p=0.07).

4.3.1.1 Reflections

The findings of this study demonstrated *in vivo* for the first time that in early PD patients there is a prominent reduction of DAT availability at pre-synaptic terminal level (putamen>caudate>ventral striatum) and to a less extent in the substantia nigra where the cell bodies are located. Moreover, the DAT binding measured along the dopaminergic projections seem to be less affected in early PD patients without clear distinctions compared to healthy control subjects.

The described molecular pattern partially confirms some preclinical and post-mortem evidences that support the hypothesis of a primary involvement of synapses and pre-terminal axons in the neurodegenerative process of PD followed by a “retrograde” degeneration of cell bodies (60,61,149). Following this hypothesis one might expect an involvement of axons preceding that of cell bodies in the substantia nigra. The findings of this study showed that DAT along the axons is preserved to a similar or larger extent than the DAT in the cell bodies. The relative preservation along nigro-striatal projections might be explained also with a compensatory up-regulation of the DAT along the axons in presence of severe pre-terminal degeneration (150).

From a learning perspective, this paper was very important for me because I was independently responsible for most of the methodological and organizational aspects of the study. In addition, through a serendipitous discovery of the presence of [^{18}F]FE-PE2I binding along the nigro-striatal projections, I was able to acquire additional knowledge on the anatomical and topographical distribution of the nigro-striatal tracts across species.

4.4 PAPER IV

4.4.1 Age related reduction of PDE10A availability in the basal ganglia

The aim of this study was to evaluate the availability of PDE10A measured with the PET radioligand [^{18}F]MNI-659 in relation to age-related and/or volumetric changes. These changes along with the limited resolution of PET might lead to inaccurate quantitative measures of target availability. In order to improve the accuracy of the quantification, in the present study the effect of age on PDE10A availability and on the volumes in the basal ganglia was performed using the HRRT system, high resolution MRI and PVE correction (methodology described in section **3.5**). $D_{2/3}$ receptor imaging was used as supplementary reference basal ganglia PET biomarker. This evaluation was conducted in 40 healthy control subjects (age 44±11, age range 27-69). The PET outcome measure was BP_{ND}, estimated using 2TCM for [^{18}F]MNI-659 (PDE10A) (described in section **3.4**) and SRTM for [^{11}C]raclopride ($D_{2/3}$ receptors), using the cerebellum as reference region. Time activity curves were corrected for PVEc. Age-related changes of PET and MRI outcome measures were examined using multiple linear regression analysis also including gender as covariate. The analysis showed the presence of a significant effect of age on the availability of PDE10A in the striatum with a decline rate of 8% per decade. A significant reduction of striatal structural volume was also detected (Figure 11).

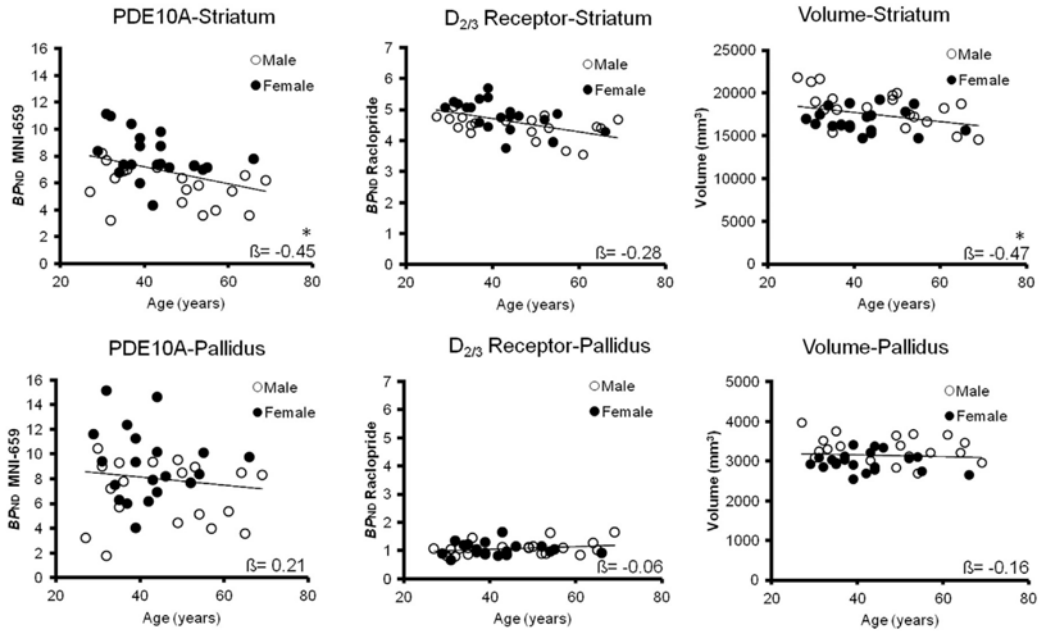

Figure 11. Correlation plots showing the relationship between age and PDE10A, Dopamine $D_{2/3}$ Receptors and volumes in the striatum and globus pallidus separated for gender. Displayed partial correlation coefficients (ß values) for the independent variable age and significance level (p) referred to the multiple regression analysis that included gender as covariate. * =$p < 0.008$ (significance after Bonferroni´s correction).

The availability of PDE10A enzyme and $D_{2/3}$ receptors were correlated in the caudate and putamen. However, a different distribution was observed in the globus pallidus and the nucleus accumbens. The availability of PDE10A was much higher than that of $D_{2/3}$ receptors in the globus pallidus. In the nucleus accumbens, negligible binding of [^{18}F]MNI-659 was observed, indicating negligible density of PDE10A, in agreement with in vitro findings observed in post-mortem autoradiography. As an additional finding, an effect of gender on PDE10A availability was also observed in the striatum ($p=0.02$).

4.4.1.1 Reflections

These results indicate that aging is associated with a considerable physiological reduction of the availability of PDE10A enzyme in the striatum. In the striatum, PDE10A availability showed a significant age-related decline that was larger compared to age-related decline of volumes measured with MRI and to the age-related decline of $D_{2/3}$ receptors availability. In the globus pallidus, a less pronounced decline of PDE10A availability was observed, whereas $D_{2/3}$ receptors availability and volumes seemed to be rather stable with aging. As a result of this analysis it appears clear that the combination of high-resolution PET and PVEc represents an advantage regarding the accuracy of PET measurements of the two molecular targets, PDE10A enzyme and $D_{2/3}$ receptors. In addition, age-matching (and for PDE10A also gender-matching) is extremely relevant in clinical PET studies which aim to examine the contribution of volume/neuronal loss (determined by age or pathology) in relation to the PDE10A and $D_{2/3}$ receptors. From a learning perspective with this study I challenged my problem solving and analytical skills with further improvement in relation to PET analysis (i.e. challenges of the kinetic analysis of [^{18}F]MNI-659 together with the application and validation of the PVCc of PET data). This paper introduced me to the analysis of MRI structural images in relation to PET outcome measures which I found stimulating and informative.

The work performed for Study IV was the methodological foundation for the clinical application performed in HDGECs in study V.

4.5 PAPER V

4.5.1 Examination of PDE10A availability across a broad spectrum of HD stages

The objective of this study was to examine the loss of PDE10A enzyme across a broad spectrum of HD stages. The study was cross-sectional with an adaptive design, examining HDGECs at different stages of the disease (early pre-manifest, late pre-manifest, stage 1 and stage 2) in comparison with control subjects matched by age and gender. Data were collected between April 4, 2013 and May 31, 2016. We obtained [^{18}F]MNI-659 and [^{11}C]raclopride PET data and MRI volumetric measurements for the following regions of interest: caudate, putamen and globus pallidus. PET data were analyzed as presented in study IV. Molecular and structural data were obtained from eighty-nine participants (44 HDGECs/45 controls) and included in the final analysis.

In each region of interest, significantly lower BP_{ND} were detected in HDGECs compared to control values. A preservation of PDE10A and $D_{2/3}$ receptors was observed in HDGECs in the early pre-manifest stage. A differential pattern of PDE10A and $D_{2/3}$ receptor loss in striatum and globus pallidus of HDGECs was observed. At manifest stages (Stage 1) PDE10A loss was larger than that of $D_{2/3}$ receptor. A plateau of PDE10A and $D_{2/3}$ receptors loss was reached from stage 1 to stage 2 (Figure 12).

Both PDE10A and $D_{2/3}$ availabilities were predictive of disease burden score.

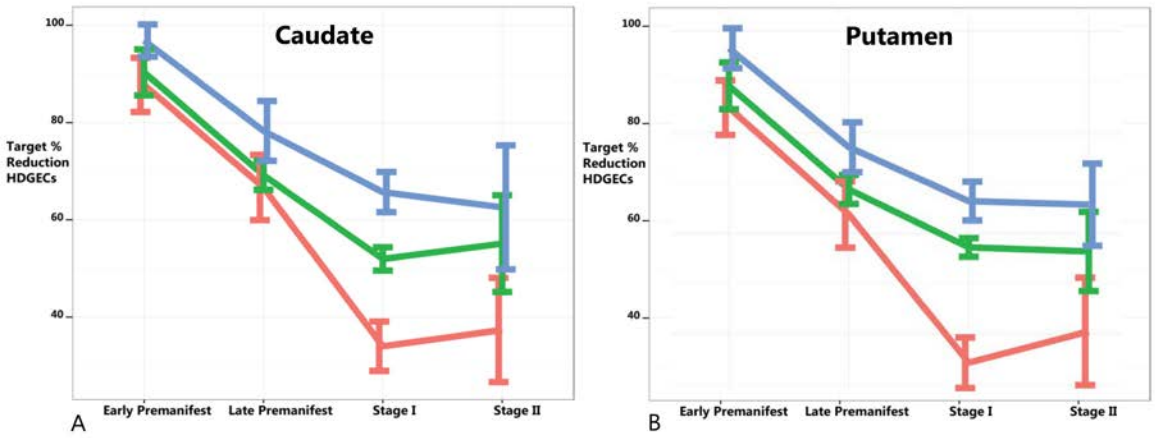

Figure 12. Percentage differences between HDGECs and HCs in the caudate (A) and putamen (B) for PDE10A enzyme (red), $D_{2/3}$ receptors (green), and volumes (blue) in the defined pre-manifest and manifest stages. Percentage differences were calculated for each HDGECs sub-group relative to its age- and gender-matched controls subgroup.

4.5.1.1 Reflections

The first interesting finding of this study was that in the early pre-manifest HDGECs group (see table 2 in section **3.7**) PDE10A, $D_{2/3}$ receptors and structural volumes did not differ from those measured in healthy controls. Between such early pre-manifest stage and the late pre-manifest stage an apparent molecular and structural phenotypic conversion begins and this might be relevant for the application of potential neuroprotective treatments. Another novel and interesting findings is that the transition between late pre-manifest and stage 1 appears to show a "turning point". In particular, it seems that during this late pre-manifest stage the decrease of PDE10A occurs at a larger rate as compared with $D_{2/3}$ receptors and striatal volumes and this is relevant because potentially indicates the suitability of PDE10A imaging as a sensitive biomarker of disease progression. Finally, when HDGECs reach stage 1-2, the decrease of PDE10A, $D_{2/3}$ receptors and volumes seems to be so pronounced that probably an intervention at this stage might not effectively modify the disease course.

There are some considerations to be done regarding PDE10A imaging and the radioligand [^{18}F]MNI-659 since the outcome measures obtained were highly variable between individuals (healthy controls and HDGECs). Part of the variability might be related to some extent to the characteristics of the radioligand but also linked to a functional intrinsic molecular inter-individual variability of the target per se. PDE10A enzyme is intracellular and can undergo different compartimentalization in the cytoplasma and Golgi complex or exists in different activation states (active or hyperactive). Therefore, the binding of [^{18}F]MNI-659 might be influenced by differences in the intra-cellular environment or activation state of the enzyme across subjects, partly contributing to the observed variability of the measured PDE10A availability.

From a learning perspective this study introduced me to the field of Huntington's disease and the efforts employed in this study by so many experts was a teaching experience about professionalism. The study has accompanied me during almost the entire PhD (between 2013-2016) period so in a way the results came along together with increased knowledge of the disease and improved personal skills. From an individual perspective this study allowed me to know personally a broad number of individuals affected by the mutation for the HD gene and this was an important motivation to carry on the efforts to successfully complete the clinical study.

5 FUTURE PERSPECTIVES

5.1.1.1 The use [^{18}F]FE-PE2I as potential clinical biomarker

Early differential diagnosis of PD is challenging with a misdiagnosis rate as high as 20–30 %. Parkinsonism as defined by UK brain bank criteria is not sufficient to assign a "diagnostic label" of sporadic PD or to recognize other atypical parkinsonian conditions such as progressive supranuclear palsy (PSP) multiple system atrophy (MSA), corticobasal degeneration (CBD) and Lewy-body dementia. Misdiagnosis is so common because of the absence of a lack of reliable biological biomarkers. [^{18}F]FE-PE2I might represent a potentially valuable tool that can help increase diagnostic specificity for dopamine-deficient parkinsonian syndromes and rationalize management decisions at initial stages of disease since it has demonstrated to be capable to evaluate the DAT availability in altered nigral structure and striatal dopamine terminals.

Different patterns of degeneration may characterize the mentioned different conditions in regard of the nigral involvement. It has already been shown that the degree of cell loss in patients with PSP with gaze palsy compared to patients without gaze palsy is different with 40 % greater loss of neurons in the substantia nigra pars reticulata (SNr) (151). Moreover [^{18}F]FE-PE2I can become a tool to monitor disease progression or the efficacy of pharmacological intervention. Longitudinal studies are needed in order to understand the ability of the radioligand to detect the amount of DAT changes that occurred in PD at different stages in 1-2 years and to evaluate inter-individual differences in disease progression.

5.1.1.2 Phosphodiesterase 10 A imaging as a pharmacodynamic biomarker

The examination *in vivo* of PD10A as target has demonstrated interesting potential as a disease biomarker in HD. Based on the results of the studies revised in section **1.3.2.2** and the study presented in paper V the measurement of PDE10A availability can be advocated, at the moment, as a suitable molecular imaging marker in future HD trials.

For the application of PDE10 imaging in future HD trials it is necessary to apply this tool into large longitudinal studies in order to understand the sensitivity of the radioligand in detection of changes and to evaluate inter-individual differences in the disease progression. Moreover, this molecular target might be used as a tool for patient's "enrichment" so that only patients with a certain PDEA level may entry in a given clinical trial. The findings of this study might

suggest that late pre-manifest HDGECs are probably the main target group where the effect of neuroprotective interventions or disease modifying therapies could be expected.

Finally it would be interesting to study the exact role and function of PDE10 in the regulation of striatal signaling (i.e. relations with other phosfodiesterase (PDE4), with other monoaminergic systems or neurotransmitters such as GABA and Glutamate).

5.1.1.3 Future directions of the field in the study of neurodegenerative disorders

Regarding potential directions of the field outside the project and the technologies presented in this thesis, I think that there other potential relevant questions that will be soon or later answered by dedicated PET imaging studies.

In the next future, the imaging community may face an era in which dedicated biomarkers of protein aggregation (α-syn or m-HTT) may become available. Those imaging probes might shed some lights in prominent pathological features and might allow a precise monitoring of the effects of therapeutics targeting the protein misfolding process.

Moreover, the availability of dedicated radioligand for α-syn, beta amyloid and tau might be relevant to start to evaluate the complex interplay between misfolding proteins in different neurodegenerative disorders (i.e. dementias and parkinsonisms).

In the same desirable future another topic of interest would be the evaluation of the relationships between the progressive pathologic protein accumulations (i.e. lewy bodies, m-HTT) and different neuroinflammatory aspects.

Finally, I am in favor of using PET imaging as a tool to stratify patients affected by neurodegenerative disorders that, without exceptions, in the clinical practice show a marked inter-individual variability.

6 ACKNOWLEDGMENTS

This thesis is the result of four intense years of studies and I feel grateful to have had this opportunity. My gratitude goes to many beautiful sentient beings that contributed to the completion of this project and are part of my working and personal community.

I feel thankful to:

All patients that for the sake of hope and knowledge volunteered to participate in the PET studies. Without You this thesis would not have been possible.

Andrea Varrone- my main supervisor. I still remember that day when we had the first interview during which I decided to follow you. I will always admire you for your scientific insights, equanimity, integrity and humanity. It has been a privilege working and learning from you.

Lars Farde- my co-supervisor, for sharing your scientific perspectives and for sharing your extensive expertise. I thank you for the time you carefully spent to dissect and improve my manuscripts.

Per Svenningsson- my co-supervisor, for being a model of a brilliant combination of researcher and clinician. I thank you for the time you have taken to introduce me to the neurology clinic at Huddinge University Hospital.

Christer Halldin- my co-supervisor, for your experienced charisma, good humor and for being always available. I thank you for the immense work performed in the field of radiochemistry and for the excellent radioligands developed.

Nina Knave, Karin Olsson, Opokua Britton Cavaco for taking good care of all individuals that performed the PET experiments included in this thesis and for the timeless emotive-practical supports. It was and it is a pleasure to work with you.

Old and new generation of radiochemists, QP, QA and affiliated that every day produce and carefully control what we inject into sentient beings. They are the engine of the PET center and I thank you for the time spent together in one way or another: *Sangram Nag, Henrik Alfredeen, Zhisheng Jia, Vladimir Stepanov, Guennadi Jogolev, Johan Ulhin, Arsalan Amir, Mahabuba Jahan, Youssef El Khoury, Mohammed Mahdi Moein, Magnus Schou, , Anne Byström, Emma Meyer, Prodip Datta* and *Carsten Steiger*

Collaborators involved in the recruitment of HDGECs: *Anna Lena Wettherholm, Per Svenningsson, Martin Paucar, Jimmy Sundblom, Dag Nyholm, Håkan Widner, Arvid Heiberg, Jan Frich, Jorge Nielsen, Lena Hjermind* and *Raymund Roos*.

All the dedicated and talented research collaborators at CHDI with whom I had the opportunity to work within the Huntington's Project. I thank you for introducing me to the Huntington's disease scientific community: *Cristina Sampaio, Ladislav Mrzljak, Cheryl Fitzer Attas, Juliana Bronzova* and *John Warner*.

Karin Zahir for your endless, indiscriminate support and for being kind-hearted

My mentor *Laura Fratiglioni* for useful career advice and insights.

I would also thank an amount of beautiful work mates with whom I had the opportunity to share the privilege of working for science. I thank you for the unlimited scientific and emotive support and for the sounded discussion about life. For this sake I would like to thank *Martin Schain, Anton Forsberg, Pontus Plavén-Sigray, Granville Matheson* and *Emma Veldman*.

My skillfull rommates *Akhiro Takano, Kai-Chun Yang and Sjoerd Finnema* that with incredible acceptance and patience have always supported me even during the darkest days.

The autoradiografy trio *Marie Svedberg, Siv Eriksson* and *Åsa Södergren* for welcoming and introducing me to the world of autoradiography.

Göran Rosenqvist thank you for the support during the reconstruction of the PET images last summer. *Urban Hansson* thank you for being always available and supportive.

Anne Axelsson for your smile and to taking good care of the PETsystem room.

All the past and current colleagues at the PET center that have supported me during the course of this PhD in so many different ways. I'm thankful for your help during those years. *Zsolt Cselény* for being a invaluable source of methodological knowledge, *Katarina Värnas* for being generous and knowledgeable, *Per Stenkrona* for the help with PET experiments and with psychiatry interviews of the research participants, *Karin Collste* for sharing all final PhD emotions, *Simon Cervenka* for friendly chats and bright views, *Johan Lundberg* for your good nature and useful suggestions, *Jenny Häggvist* for inspiring discussions, *Aurelija Jucaite* for sharing the joy and pain of life occurrences and *Miklós Tóth* for your ironic touch, *Balazs Gulyas* for your interesting insight, *Mikael Tiger* for being always kind, *Marcello Venzi* for our "scientific" friendship and for the help with nice graphs.

Other members of the group that made the time here more pleasurable: *Max Andersson, Junya Matsumoto, Ämma Tangen, Kia Hultberg-Lundberg, Jonas Ahlgren, Jacqueline Borg, Peter Johnström, Lenke Tari, Patrik Mattsson, Malen Kjellen, Pauliina Ikonen, Sara Lundqvist, Petra Agirman, Ida Sonni, Davide d'Arienzo* and *Jonas Svensson*.

Daniel Ferreira Padilla for friendship and for taking your time to introduce me to Freesurfer

My first scientific life mentor *Enrico Granieri.*

Our new community of friends in Stockholm and in particular *Marco, Ingrid, Ida* and *Anna Rivetti* for your endless support and pure friendship.

My parents *Eva* e *Mario* that have supported me for so many years.

Nina and *Zeno* for grounding me to the mother earth with a different perspective

I thank you ***Giulia*** for your love, compassion, and unique humanity. For showing and sharing me your understanding beyond schemas and for being my companion in this life journey.

7 REFERENCES

1. Bolam JP, Hanley JJ, Booth P a, Bevan MD. Synaptic organisation of the basal ganglia. J Anat. 2000;196 (Pt 4):527–42.

2. Gerfen CR, Bolam JP. The Neuroanatomical Organization of the Basal Ganglia. Handbook of Behavioral Neuroscience. Elsevier Inc.; 2017. 3-32 p.

3. Alexander GE, Crutcher MD. Functional architecture of basal ganglia circuits: neural substrates of parallel processing. Trends Neurosci. 1990 Jul;13(7):266–71.

4. Albin RL, Young AB, Penney JB. The functional anatomy of disorders of the basal ganglia. Trends Neurosci. 1995 Feb;18(2):63–4.

5. Calabresi P, Picconi B, Tozzi A, Ghiglieri V, Di Filippo M. Direct and indirect pathways of basal ganglia: a critical reappraisal. Nat Neurosci. 2014 Aug;17(8):1022–30.

6. Nambu A. Seven problems on the basal ganglia. Curr Opin Neurobiol. 2008 Dec;18(6):595–604.

7. Haber SN. Corticostriatal circuitry. Dialogues Clin Neurosci. 2016 Mar;18(1):7–21.

8. Worbe Y, Baup N, Grabli D, Chaigneau M, Mounayar S, McCairn K, et al. Behavioral and movement disorders induced by local inhibitory dysfunction in primate striatum. Cereb Cortex. 2009 Aug;19(8):1844–56.

9. Tremblay L, Worbe Y, Thobois S, Sgambato-Faure V, Feger J. Selective dysfunction of basal ganglia subterritories: From movement to behavioral disorders. Mov Disord. 2015 Aug;30(9):1155–70.

10. Ztaou S, Maurice N, Camon J, Guiraudie-Capraz G, Kerkerian-Le Goff L, Beurrier C, et al. Involvement of Striatal Cholinergic Interneurons and M1 and M4 Muscarinic Receptors in Motor Symptoms of Parkinson's Disease. J Neurosci. 2016 Aug;36(35):9161–72.

11. Beggiato S, Tomasini MC, Borelli AC, Borroto-Escuela DO, Fuxe K, Antonelli T, et al. Functional role of striatal A2A, D2, and mGlu5 receptor interactions in regulating striatopallidal GABA neuronal transmission. J Neurochem. 2016 Jul;138(2):254–64.

12. Brimblecombe KR, Cragg SJ. Substance P Weights Striatal Dopamine Transmission Differently within the Striosome-Matrix Axis. J Neurosci. 2015 Jun;35(24):9017–23.

13. Salinas AG, Davis MI, Lovinger DM, Mateo Y. Dopamine dynamics and cocaine sensitivity differ between striosome and matrix compartments of the striatum. Neuropharmacology. 2016 Sep;108:275–83.

14. Nambu A, Tokuno H, Takada M. Functional significance of the cortico-subthalamo-pallidal 'hyperdirect' pathway. Neurosci Res. 2002 Jun;43(2):111–7.

15. Oswal A, Brown P, Litvak V. Synchronized neural oscillations and the pathophysiology of Parkinson's disease. Curr Opin Neurol. 2013 Dec;26(6):662–70.

16. Cagnan H, Duff EP, Brown P. The relative phases of basal ganglia activities dynamically shape effective connectivity in Parkinson's disease. Brain. 2015

Jun;138(Pt 6):1667–78.

17. Crossman AR, Obeso JA. Functions of the basal ganglia-paradox or no paradox? Mov Disord. 2016 Aug;31(8):1120–1.

18. Marsden CD, Obeso JA. The functions of the basal ganglia and the paradox of stereotaxic surgery in Parkinson's disease. Brain. 1994 Aug;117 (Pt 4:877–97.

19. Dale AM, Fischl B, Sereno MI. Cortical surface-based analysis. I. Segmentation and surface reconstruction. Neuroimage. 1999;9(2):179–94.

20. Fischl B, Salat DH, Kouwe AJW Van Der, Makris N, Quinn BT, Dale AM. Sequence-independent Segmentation of Magnetic Resonance Images. Neuroimage. 2004;23(Suppl1):S69–84.

21. Fischl B, Salat DH, Busa E, Albert M, Dieterich M, Haselgrove C, et al. Whole Brain Segmentation: Neurotechnique Automated Labeling of Neuroanatomical Structures in the Human Brain. Neuron. 2002;33(3):341–55.

22. Carson RE. Tracer Kinetic Modeling in PET. In: Bailey DL, Townsend DW, Valk PE, Maisey MN, editors. Positron Emission Tomography: Basic Sciences. Springer London; 2005. p. 127–59.

23. Lammertsma AA, Hume SP. Simplified reference tissue model for PET receptor studies. Neuroimage. 1996 Dec;4(3 Pt 1):153–8.

24. Logan J, Fowler JS, Volkow ND, Wolf AP, Dewey SL, Schlyer DJ, et al. Graphical analysis of reversible radioligand binding from time-activity measurements applied to [N-11C-methyl]-(-)-cocaine PET studies in human subjects. J Cereb Blood Flow Metab. 1990 Sep;10(5):740–7.

25. Cselényi Z, Olsson H, Halldin C, Gulyás B, Farde L. A comparison of recent parametric neuroreceptor mapping approaches based on measurements with the high affinity PET radioligands [11C]FLB 457 and [11C]WAY 100635. Neuroimage. 2006 Oct 1;32(4):1690–708.

26. Schain M, Tóth M, Cselényi Z, Arakawa R, Halldin C, Farde L, et al. Improved mapping and quantification of serotonin transporter availability in the human brainstem with the HRRT. Eur J Nucl Med Mol Imaging. 2013;40:228-37.

27. Higuchi M, Trojanowski JQ. Pathobiological features in neurodegenerative diseases: an overview.Inter Cong Series 2004;1260:69–75.

28. Jones L, Houlden H, Tabrizi SJ. DNA repair in the trinucleotide repeat disorders. Lancet Neurol. Elsevier Ltd; 2017;16(1):88–96.

29. Olanow CW, Kordower JH. Targeting α-Synuclein as a therapy for Parkinson's disease: The battle begins. Mov Disord. 2017;32(2):203–7.

30. Wong YC, Krainc D. α -synuclein toxicity in neurodegeneration : mechanism and therapeutic strategies. Nat Neuroscience. 2017;23(2):1–13.

31. Schenk DB, Koller M, Ness DK, Griffith SG, Grundman M, Zago W, et al. First-in-human assessment of PRX002, an anti-alpha-synuclein monoclonal antibody, in healthy volunteers. Mov Disord. 2017 Feb;32(2):211–8.

32. Kay C, Collins JA, Skotte NH, Southwell AL, Warby SC, Caron NS, et al. Huntingtin

Haplotypes Provide Prioritized Target Panels for Allele-specific Silencing in Huntington Disease Patients of European Ancestry. Mol Ther. American Society of Gene & Cell Therapy; 2015;23(11):1759–71.

33. Weir DW, Sturrock A, Leavitt BR. Development of biomarkers for Huntington's disease. Lancet Neurol. 2011;10(6):573–90.

34. Ross CA, Aylward EH, Wild EJ, Langbehn DR, Long JD, Warner JH, et al. Huntington disease: natural history, biomarkers and prospects for therapeutics. Nat Rev Neurol. 2014 Apr;10(4):204–16.

35. Postuma RB, Berg D. Advances in markers of prodromal Parkinson disease. Nat Rev Neurol. 2016;12(11):622–34.

36. Espay AJ, Schwarzschild MA, Tanner CM, Fernandez HH, Simon DK, Leverenz JB, et al. Biomarker-driven phenotyping in Parkinson's disease: A translational missing link in disease-modifying clinical trials. Mov Disord. 2017;0(0):1–6.

37. Lesage S, Brice A. Parkinson's disease: from monogenic forms to genetic susceptibility factors. Hum Mol Genet. 2009 Apr;18(R1):R48-59.

38. Scheperjans F, Pekkonen E, Kaakkola S, Auvinen P. Linking Smoking, Coffee, Urate, and Parkinson's Disease - A Role for Gut Microbiota? J Parkinsons Dis. 2015;5(2):255–62.

39. Scheperjans F, Aho V, Pereira PAB, Koskinen K, Paulin L, Pekkonen E, et al. Gut microbiota are related to Parkinson's disease and clinical phenotype. Mov Disord. 2015 Mar;30(3):350–8.

40. Bonifati V. Genetics of Parkinson's disease--state of the art, 2013. Parkinsonism Relat Disord. 2014 Jan;20 Suppl 1:S23-8.

41. Davis AA, Andruska KM, Benitez BA, Racette BA, Perlmutter JS, Cruchaga C. Variants in GBA, SNCA, and MAPT influence Parkinson disease risk, age at onset, and progression. Neurobiol Aging. 2016 Jan;37:209.e1-7.

42. Alcalay RN, Levy OA, Waters CC, Fahn S, Ford B, Kuo S-H, et al. Glucocerebrosidase activity in Parkinson's disease with and without GBA mutations. Brain. 2015 Sep;138(Pt 9):2648–58.

43. Kalia L V, Lang AE, Hazrati LN, Fujioka S, Wszolek ZK, Dickson DW, et al. Clinical correlations with Lewy body pathology in LRRK2-related Parkinson disease. JAMA Neurol. 2015;72(1):100–5.

44. Wirdefeldt K, Adami H, Cole P, Trichopoulos D, Mandel J. Epidemiology and etiology of Parkinson's disease: a review of the evidence. Eur J Epidemiol suppl 2011;26:S1-58.

45. Von Campenhausen S, Bornschein B, Wick R, Bötzel K, Sampaio C, Poewe W, et al. Prevalence and incidence of Parkinson's disease in Europe. Eur Neuropsychopharmacol. 2005;15(4):473–90.

46. de Lau LML, Breteler MMB. Epidemiology of Parkinson's disease. Lancet Neurol. 2006 Jun;5(6):525–35.

47. Lökk J, Borg S, Svensson J, Persson U, Ljunggren G. Drug and treatment costs in

Parkinson’s disease patients in Sweden. Acta Neurol Scand. 2012;125(2):142–7.

48. Dorsey ER, Constantinescu R, Thompson JP, Biglan KM, Holloway RG, Kieburtz K, et al. Projected number of people with Parkinson disease in the most populous nations, 2005 through 2030. Neurology. 2007 Jan;68(5):384–6.

49. Jellinger K a. The pathomechanisms underlying Parkinson’s disease. Expert Rev Neurother. 2014;14:199–215.

50. Braak H, Del Tredici K, Rub U, de Vos RAI, Jansen Steur ENH, Braak E. Staging of brain pathology related to sporadic Parkinson’s disease. Neurobiol Aging. 2003;24(2):197–211.

51. Del Tredici K, Braak H. Review: Sporadic Parkinson’s disease: development and distribution of alpha-synuclein pathology. Neuropathol Appl Neurobiol. 2016 Feb;42(1):33–50.

52. Jellinger KA. Formation and development of Lewy pathology: A critical update. J Neurol. 2009;256 (Suppl. 3):270–9.

53. Braak H, Del Tredici K. Neuropathological Staging of Brain Pathology in Sporadic Parkinson’s disease: Separating the Wheat from the Chaff. J Parkinsons Dis. 2017;7(s1):S73–87.

54. Pacelli C, Giguere N, Bourque M-J, Levesque M, Slack RS, Trudeau L-E. Elevated Mitochondrial Bioenergetics and Axonal Arborization Size Are Key Contributors to the Vulnerability of Dopamine Neurons. Curr Biol. 2015 Sep;25(18):2349–60.

55. Giguere N, Trudeau L-E. Axon arborization size is a key factor influencing cellular bioenergetics and vulnerability of dopamine neurons in Parkinson’s disease. Med Sci (Paris). 2016 Apr;32(4):342–4.

56. Surmeier DJ, Obeso JA, Halliday GM. Selective neuronal vulnerability in Parkinson disease. Nat Rev Neurosci. 2017;18(2): 101-113.

57. Gibb WR, Lees AJ. The relevance of the Lewy body to the pathogenesis of idiopathic Parkinson’s disease. J Neurol Neurosurg Psychiatry. 1988;51(6):745–52.

58. Kordower JH, Olanow CW, Dodiya HB, Chu Y, Beach TG, Adler CH, et al. Disease duration and the integrity of the nigrostriatal system in Parkinson’s disease. Brain. 2013;136(8):2419–31.

59. Burke RE, O’Malley K. Axon degeneration in Parkinson’s disease. Exp Neurol. 2013;246:72–83.

60. Kordower JH, Olanow CW, Dodiya HB, Chu Y, Beach TG, Adler CH, et al. Disease duration and the integrity of the nigrostriatal system in Parkinson’s disease. Brain. 2013;136:2419–31.

61. Cheng HC, Ulane C., Burke R. Clinical progression in Parkinson’s disease and the neurobiology of Axons. Ann Neurol. 2010;67(6):715–25.

62. Snow BJ, Tooyama I, McGeer EG, Yamada T, Calne DB, Takahashi H, et al. Human positron emission tomographic [18F]fluorodopa studies correlate with dopamine cell counts and levels. Ann Neurol. 1993 Sep;34(3):324–30.

63. Brooks DJ, Pavese N. Imaging biomarkers in Parkinson’s disease. Prog Neurobiol.

2011;95(4):614–28.

64. Sossi V, de la Fuente-Fernandez R, Holden JE, Schulzer M, Ruth TJ, Stoessl J. Changes of dopamine turnover in the progression of Parkinson's disease as measured by positron emission tomography: their relation to disease-compensatory mechanisms. J Cereb Blood Flow Metab. 2004 Aug;24(8):869–76.

65. Storch A, Wolz M, Beuthien-Baumann B, Lohle M, Herting B, Schwanebeck U, et al. Effects of dopaminergic treatment on striatal dopamine turnover in de novo Parkinson disease. Neurology. 2013 May;80(19):1754–61.

66. Martin WRW, Wieler M, Stoessl AJ, Schulzer M. Dihydrotetrabenazine positron emission tomography imaging in early, untreated Parkinson's disease. Ann Neurol. 2008 Mar;63(3):388–94.

67. Hsiao I-T, Weng Y-H, Hsieh C-J, Lin W-Y, Wey S-P, Kung M-P, et al. Correlation of Parkinson disease severity and 18F-DTBZ positron emission tomography. JAMA Neurol 2014;71(6):758–66.

68. Lee CS, Samii A, Sossi V, Ruth TJ, Schulzer M, Holden JE, et al. In vivo positron emission tomographic evidence for compensatory changes in presynaptic dopaminergic nerve terminals in Parkinson's disease. Ann Neurol. 2000;47(4):493–503.

69. Kilbourn MR, Butch ER, Desmond T, Sherman P, Harris PE, Frey KA. In vivo [11C]dihydrotetrabenazine binding in rat striatum: sensitivity to dopamine concentrations. Nucl Med Biol. 2010 Jan;37(1):3–8.

70. Catafau AM, Tolosa E. Impact of dopamine transporter SPECT using 123I-Ioflupane on diagnosis and management of patients with clinically uncertain Parkinsonian syndromes. Mov Disord. 2004 Oct;19(10):1175–82.

71. Benamer HT, Patterson J, Wyper DJ, Hadley DM, Macphee GJ, Grosset DG. Correlation of Parkinson's disease severity and duration with 123I-FP-CIT SPECT striatal uptake. Mov Disord. 2000 Jul;15(4):692–8.

72. Marek KL, Seibyl JP, Zoghbi SS, Zea-Ponce Y, Baldwin RM, Fussell B, et al. [123I] beta-CIT/SPECT imaging demonstrates bilateral loss of dopamine transporters in hemi-Parkinson's disease. Neurology. 1996 Jan;46(1):231–7.

73. Jennings DL, Seibyl JP, Oakes D, Eberly S, Murphy J, Marek K. (123I) beta-CIT and single-photon emission computed tomographic imaging vs clinical evaluation in Parkinsonian syndrome: unmasking an early diagnosis. Arch Neurol. 2004 Aug;61(8):1224–9.

74. Erro R, Schneider SA, Stamelou M, Quinn NP, Bhatia KP. What do patients with scans without evidence of dopaminergic deficit (SWEDD) have? New evidence and continuing controversies. J Neurol Neurosurg Psychiatry. 2016 Mar;87(3):319–23.

75. Ling H, Kearney S, Yip HLK, Silveira-Moriyama L, Revesz T, Holton JL, et al. Parkinson's disease without nigral degeneration: a pathological correlate of scans without evidence of dopaminergic deficit (SWEDD)? J Neurol Neurosurg Psychiatry. 2016 Jun;87(6):633–41.

76. Wile DJ, Dinelle K, Vafai N, McKenzie J, Tsui JK, Schaffer P, et al. A scan without evidence is not evidence of absence: Scans without evidence of dopaminergic deficit

in a symptomatic leucine-rich repeat kinase 2 mutation carrier. Mov Disord. 2016 Mar;31(3):405–9.

77. Varrone A, Halldin C. Molecular imaging of the dopamine transporter. J Nucl Med. 2010;51(9):1331–4.

78. Strafella AP, Bohnen NI, Perlmutter JS, Eidelberg D, Pavese N, Van Eimeren T, et al. Molecular imaging to track Parkinson's disease and atypical parkinsonisms: New imaging frontiers. Mov Disord. 2017;32(2):181–92.

79. Varrone A, Pappatà S, Quarantelli M. Movement Disorders: Focus on Parkinson's Disease and Related Disorders. In: Ciarmiello A, Mansi L, editors. PET-CT and PET-MRI in Neurology: SWOT Analysis Applied to Hybrid Imaging. Cham: Springer International Publishing; 2016. p. 103–25.

80. Brooks DJ. Examining Braak's hypothesis by imaging Parkinson's disease. Mov Disord. 2010; 25 Suppl 1:S83-8.

81. Gallagher CL, Oakes TR, Johnson SC, Chung MK, Holden JE, Bendlin BB, et al. Rate of 6-[18F]fluorodopa uptake decline in striatal subregions in Parkinson's disease. Mov Disord. 2011 Mar;26(4):614–20.

82. Morrish PK, Sawle G V, Brooks DJ. An [18F]dopa-PET and clinical study of the rate of progression in Parkinson's disease. Brain. 1996 Apr;119 (Pt 2:585–91.

83. Nurmi E, Ruottinen HM, Kaasinen V, Bergman J, Haaparanta M, Solin O, et al. Progression in Parkinson's disease: a positron emission tomography study with a dopamine transporter ligand [18F]CFT. Ann Neurol. 2000 Jun;47(6):804–8.

84. Nandhagopal R, Kuramoto L, Schulzer M, Mak E, Cragg J, Lee CS, et al. Longitudinal progression of sporadic Parkinson's disease: a multi-tracer positron emission tomography study. Brain. 2009 Nov;132(Pt 11):2970–9.

85. Varrone A, Steiger C, Schou M, Takano A, Finnema SJ, Guilloteau D, et al. In vitro autoradiography and in vivo evaluation in cynomolgus monkey of [18F]FE-PE2I, a new dopamine transporter PET radioligand. Synapse. 2009;63(10):871–80.

86. Sasaki T, Ito H, Kimura Y, Arakawa R, Takano H, Seki C, et al. Quantification of Dopamine Transporter in Human Brain Using PET with 18F-FE-PE2I. J Nucl Med. 2012;53:1065–73.

87. Brooks DJ, Ibanez V, Sawle G V, Playford ED, Quinn N, Mathias CJ, et al. Striatal D2 receptor status in patients with Parkinson's disease, striatonigral degeneration, and progressive supranuclear palsy, measured with 11C-raclopride and positron emission tomography. Ann Neurol. 1992 Feb;31(2):184–92.

88. Antonini A, Leenders KL, Vontobel P, Maguire RP, Missimer J, Psylla M, et al. Complementary PET studies of striatal neuronal function in the differential diagnosis between multiple system atrophy and Parkinson's disease. Brain. 1997 Dec;120 (Pt 1):2187–95.

89. Antonini A, Schwarz J, Oertel WH, Pogarell O, Leenders KL. Long-term changes of striatal dopamine D2 Receptors in patients with Parkinson's disease: A study with positron emission tomography and [11C]Raclopride. Mov Disord. Wiley Subscription Services, Inc., A Wiley Company; 1997;12(1):33–8.

90. Scherfler C, Khan NL, Pavese N, Lees AJ, Quinn NP, Brooks DJ, et al. Upregulation of dopamine D2 receptors in dopaminergic drug-naive patients with Parkin gene mutations. Mov Disord. 2006;21(6):783–8.

91. Huot P, Fox SH. The serotonergic system in motor and non-motor manifestations of Parkinson's disease. Exp Brain Res. 2013;

92. Halliday GM, Li YW, Blumbergs PC, Joh TH, Cotton RG, Howe PR, et al. Neuropathology of immunohistochemically identified brainstem neurons in Parkinson's disease. Ann Neurol. 1990 Apr;27(4):373–85.

93. Kish SJ, Tong J, Hornykiewicz O, Rajput A, Chang L-J, Guttman M, et al. Preferential loss of serotonin markers in caudate versus putamen in Parkinson's disease. Brain. 2008 Jan;131(Pt 1):120–31.

94. Ng KY, Colburn RW, Kopin IJ. Effects of L-dopa on efflux of cerebral monoamines from synaptosomes. Nature. 1971 Apr;230(5292):331–2.

95. Kerenyi L, Ricaurte GA, Schretlen DJ, McCann U, Varga J, Mathews WB, et al. Positron emission tomography of striatal serotonin transporters in Parkinson disease. Arch Neurol. 2003 Sep;60(9):1223–9.

96. Guttman M, Boileau I, Warsh J, Saint-Cyr JA, Ginovart N, McCluskey T, et al. Brain serotonin transporter binding in non-depressed patients with Parkinson's disease. Eur J Neurol. 2007 May;14(5):523–8.

97. Boileau I, Warsh JJ, Guttman M, Saint-Cyr JA, McCluskey T, Rusjan P, et al. Elevated serotonin transporter binding in depressed patients with Parkinson's disease: a preliminary PET study with [11C]DASB. Mov Disord. 2008 Sep;23(12):1776–80.

98. Politis M, Wu K, Loane C, Kiferle L, Molloy S, Brooks DJ, et al. Staging of serotonergic dysfunction in Parkinson's Disease: An in vivo 11C-DASB PET study. Neurobiol Dis. 2010;

99. Albin RL, Koeppe RA, Bohnen NI, Wernette K, Kilbourn MA, Frey KA. Spared caudal brainstem SERT binding in early Parkinson's disease. J Cereb Blood Flow Metab. 2008 Mar;28(3):441–4.

100. Eddy CM, Parkinson EG, Rickards HE. Changes in mental state and behaviour in Huntington's disease. The lancet Psychiatry. 2016 Nov;3(11):1079–86.

101. MacDonald ME, Ambrose CM, Duyao MP, Myers RH, Lin C, Srinidhi L, et al. A novel gene containing a trinucleotide repeat that is expanded and unstable on Huntington's disease chromosomes. Cell. 1993;72(6):971–83.

102. Landwehrmeyer GB, McNeil SM, Dure LS, Ge P, Aizawa H, Huang Q, et al. Huntington's disease gene: Regional and cellular expression in brain of normal and affected individuals. Ann Neurol. 1995;37(2):218–30.

103. Pringsheim T, Wiltshire K, Day L, Dykeman J, Steeves T, Jette N. The incidence and prevalence of Huntington's disease: A systematic review and meta-analysis. Mov Disord. 2012;27(9):1083–91.

104. Rawlins MD, Wexler NS, Wexler AR, Tabrizi SJ, Douglas I, Evans SJW, et al. The prevalence of huntington's disease. Neuroepidemiology. 2016;46(2):144–53.

105. Wexler NS, Lorimer J, Porter J, Gomez F, Moskowitz C, Shackell E, et al. Venezuelan kindreds reveal that genetic and environmental factors modulate Huntington's disease age of onset. Proc Natl Acad Sci U S A. 2004 Mar;101(10):3498–503.

106. Paulsen JS, Long JD, Ross CA, Harrington DL, Erwin CJ, Williams JK, et al. Prediction of manifest huntington's disease with clinical and imaging measures: A prospective observational study. Lancet Neurol. 2014;13(12):1193–201.

107. Lee JM, Wheeler VC, Chao MJ, Vonsattel JPG, Pinto RM, Lucente D, et al. Identification of Genetic Factors that Modify Clinical Onset of Huntington's Disease. Cell. 2015;162(3):516–26.

108. Dorsey ER. Natural history of Huntington disease. JAMA Neurol 2013;70:1520–30. 3

109. Saudou F, Humbert S. The Biology of Huntingtin. Neuron 2016;89(5):919-26.

110. Mcfarland KN, Cha J-HJ. Chapter 3 - Molecular biology of Huntington's disease. 1st ed. Hyperkinetic Movement Disorders. Elsevier B.V.; 2011. 25-81 p.

111. Vonsattel JPG, Keller C, Cortes Ramirez EP. Huntington's disease - neuropathology. 1st ed. Handbook of Clinical Neurology. Elsevier B.V.; 2011. 83-100 p.

112. Glass M, Dragunow M, Faull RLM. The pattern of neurodegeneration in Huntington's disease: A comparative study of cannabinoid, dopamine, adenosine and GABA(A) receptor alterations in the human basal ganglia in Huntington's disease. Neuroscience. 2000;97(3):505–19.

113. Allen KL, Waldvogel HJ, Glass M, Faull RLM. Cannabinoid (CB1), GABAA and GABAB receptor subunit changes in the globus pallidus in Huntington's disease. J Chem Neuroanat. 2009;37(4):266–81.

114. Seidel K, Heinsen H, Vonsattel JP, Dunnen WF Den, Korf HW. Huntington ' s disease (HD): the neuropathology of a multisystem neurodegenerative disorder of the human brain. 2016;26:726–40.

115. Rüb U, Hentschel M, Stratmann K, Brunt E, Heinsen H, Seidel K, et al. Huntington's disease (HD): Degeneration of select nuclei, widespread occurrence of neuronal nuclear and axonal inclusions in the brainstem. Brain Pathol. 2014;24(3):247–60.

116. Heinsen H, Rüb U, Gangnus D, Jungkunz G, Bauer M, Ulmar G, et al. Nerve cell loss in the thalamic centromedian-parafascicular complex in patients with Huntington's disease. Acta Neuropathol. 1996;91(2):161–8.

117. Ginovart N, Lundin A, Farde L, Halldin C, Bäckman L, Swahn CG, et al. PET study of the pre- and post-synaptic dopaminergic markers for the neurodegenerative process in Huntington's disease. Brain. 1997;120(3):503–14.

118. Turjanski N, Weeks R, Dolan R, Harding AE, Brooks DJ. Striatal D1 and D2 receptor binding in patients with Huntington's disease and other choreas. A PET study. Brain. 1995 Jun;118:689–96.

119. Andrews TC, Weeks RA, Turjanski N, Gunn RN, Watkins LH, Sahakian B, et al. Huntington's disease progression. PET and clinical observations. Brain. 1999;122:2353–63.

120. Antonini A, Leenders KL, Spiegel R, Meier D, Vontobel P, Weigell-Weber M, et al.

Striatal glucose metabolism and dopamine D2 receptor binding in asymptomatic gene carriers and patients with Huntington's disease. Brain. 1996 Dec;119 (Pt 6:2085–95.

121. Sanchez-Pernaute R, Kunig G, del Barrio Alba A, de Yebenes JG, Vontobel P, Leenders KL. Bradykinesia in early Huntington's disease. Neurology. 2000 Jan;54(1):119–25.

122. van Oostrom JCH, Maguire RP, Verschuuren-Bemelmans CC, Veenma-van der Duin L, Pruim J, Roos RAC, et al. Striatal dopamine D2 receptors, metabolism, and volume in preclinical Huntington disease. Neurology. 2005 Sep;65(6):941–3.

123. Pavese N, Andrews TC, Brooks DJ, Ho AK, Rosser AE, Barker RA, et al. Progressive striatal and cortical dopamine receptor dysfunction in Huntington's disease: a PET study. Brain. 2003 May;126(Pt 5):1127–35.

124. Pavese N, Politis M, Tai YF, Barker RA, Tabrizi SJ, Mason SL, et al. Cortical dopamine dysfunction in symptomatic and premanifest Huntington's disease gene carriers. Neurobiol Dis. 2010 Feb;37(2):356–61.

125. Esmaeilzadeh M, Farde L, Karlsson P, Varrone A, Halldin C, Waters S, et al. Extrastriatal dopamine D(2) receptor binding in Huntington's disease. Hum Brain Mapp. 2011;32(10):1626–36.

126. Politis M, Pavese N, Tai YF, Kiferle L, Mason SL, Brooks DJ, et al. Microglial activation in regions related to cognitive function predicts disease onset in Huntington's disease: A multimodal imaging study. Hum Brain Mapp. 2011;32(2):258–70.

127. Tai YF, Pavese N, Gerhard A, Tabrizi SJ, Barker RA, Brooks DJ, et al. Microglial activation in presymptomatic Huntington's disease gene carriers. Brain. 2007 Jul;130(Pt 7):1759–66.

128. Bohnen NI, Koeppe RA, Meyer P, Ficaro E, Wernette K, Kilbourn MR, et al. Decreased striatal monoaminergic terminals in Huntington disease. Neurology. 2000 May;54(9):1753–9.

129. Wilson LS, Brandon NJ. Emerging Biology of PDE10A. Curr Pharm Des 2015;378–88.

130. Ahmad R, Bourgeois S, Postnov A, Schmidt ME, Bormans G, Van Laere K, et al. PET imaging shows loss of striatal PDE10A in patients with Huntington disease. Neurology. 2014 Jan 21;82(3):279–81.

131. Russell DS, Barret O, Jennings DL, Friedman JH, Tamagnan GD, Thomae D, et al. The Phosphodiesterase 10 Positron Emission Tomography Tracer, [18 F]MNI-659, as a Novel Biomarker for Early Huntington Disease. JAMA Neurol. 2014 1;71(12):1520.

132. Russell DS, Jennings DL, Barret O, Tamagnan GD, Carroll VM, Caille F, et al. Change in PDE10 across early Huntington disease assessed by [18F]MNI-659 and PET imaging. Neurology. 2016 Feb 23;86(8):748–54.

133. Niccolini F, Haider S, Reis Marques T, Muhlert N, Tziortzi AC, Searle GE, et al. Altered PDE10A expression detectable early before symptomatic onset in Huntington's disease. Brain. 2015;138(10):3016–29.

134. Boden R, Persson J, Wall A, Lubberink M, Ekselius L, Larsson E-M, et al. Striatal

phosphodiesterase 10A and medial prefrontal cortical thickness in patients with schizophrenia: a PET and MRI study. Transl Psychiatry. 2017 Mar;7(3):e1050.

135. Varrone A, Sjöholm N, Eriksson L, Gulyás B, Halldin C, Farde L. Advancement in PET quantification using 3D-OP-OSEM point spread function reconstruction with the HRRT. Eur J Nucl Med Mol Imaging. 2009;36(10):1639–50.

136. Hall H, Halldin C, Farde L, Sedvall G. Whole hemisphere autoradiography of the postmortem human brain. Nuclear Medicine and Biology. 1998;25(8): 715–9.

137. Varnäs K, Halldin C, Hall H. Autoradiographic distribution of serotonin transporters and receptor subtypes in human brain. Hum Brain Mapp. 2004;22(3):246–60.

138. Tian X, Vroom C, Ghofrani HA, Weissmann N, Bieniek E, Grimminger F, et al. Phosphodiesterase 10A upregulation contributes to pulmonary vascular remodeling. PLoS One. 2011;6(4):1–12.

139. Barret O, Thomae D, Tavares A, Alagille D, Papin C, Waterhouse R, et al. In Vivo Assessment and Dosimetry of 2 Novel PDE10A PET Radiotracers in Humans: 18F-MNI-659 and 18F-MNI-654. J Nucl Med. 2014;55(8):1297–304.

140. Rousset OG, Ma Y, Evans AC. Correction for partial volume effects in PET: principle and validation. J Nucl Med. 1998;39(5):904–11.

141. Rousset O, Rahmim A, Alavi A, Zaidi H. Partial Volume Correction Strategies in PET. PET Clinics. 2007;2(2): 235–49.

142. Napadow V, Dhond R, Kennedy D, Hui KKS, Makris N. Automated Brainstem Co-registration (ABC) for MRI. Neuroimage. 2006;32(3):1113–9.

143. Jenkinson M, Beckmann CF, Behrens TEJ, Woolrich MW, Smith SM. FSL. Neuroimage. 2012 15;62(2):782–90.

144. Huntington Study Group. Unified Huntington's Disease Rating Scale: Reliability - and-Consis tenc. Mov Disord.1996;11(2):136–42.

145. Schou M, Steiger C, Varrone A, Guilloteau D, Halldin C. Synthesis, radiolabeling and preliminary in vivo evaluation of [18F]FE-PE2I, a new probe for the dopamine transporter. Bioorganic Med Chem Lett. 2009;19(16):4843–5.

146. Varrone A, Gulyás B, Takano A, Stabin MG, Jonsson C, Halldin C. Simplified quantification and whole-body distribution of [18F]FE-PE2I in nonhuman primates: Prediction for human studies. Nucl Med Biol. 2012;39(2):295–303.

147. Lambert C, Chowdhury R, Fitzgerald THB, Fleming SM, Lutti A, Hutton C, et al. Characterizing aging in the human brainstem using quantitative multimodal MRI analysis. Front Hum Neurosci. 2013;7(August):462.

148. Commons KG. Two major network domains in the dorsal raphe nucleus. J Comp Neurol. 2015 Jul;523(10):1488–504.

149. Chung CY, Koprich JB, Siddiqi H, Isacson O. Dynamic changes in presynaptic and axonal transport proteins combined with striatal neuroinflammation precede dopaminergic neuronal loss in a rat model of AAV alpha-synucleinopathy. J Neurosci. 2009 Mar;29(11):3365–73.

150. Block ER, Nuttle J, Balcita-Pedicino JJ, Caltagarone J, Watkins SC, Sesack SR, et al.

Brain Region-Specific Trafficking of the Dopamine Transporter. J Neurosci. 2015;35(37):12845–58.

151. Halliday GM, Hardman CD, Cordato NJ, Hely MA, Morris JG. A role for the substantia nigra pars reticulata in the gaze palsy of progressive supranuclear palsy. Brain. 2000 Apr;123 (Pt 4):724–32.